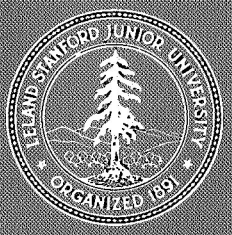

STANFORD UNIVERSITY
ENGINEERING IN MEDICINE AND BIOLOGY

TRANSMISSION CHARACTERISTICS OF DISTENSION, TORSION AND AXIAL WAVES IN ARTERIES

PH. D. DISSERTATION

BY

WILLIAM E. MORITZ

BIOMECHANICS LABORATORY

DEPARTMENT OF AERONAUTICS AND ASTRONAUTICS

SUDAAR NO. 373
MAY 1969

This work was carried out at the Ames Research Center of NASA under a collaborative research arrangement with Stanford University (NASA Grant NGR 05-020-223) and was supported in part by a NASA Traineeship. The material from SUDAAR 343 is included for completeness.

Department of Aeronautics and Astronautics
Stanford University
Stanford, California

TRANSMISSION CHARACTERISTICS OF DISTENSION, TORSION AND AXIAL WAVES IN ARTERIES

Ph.D. Dissertation

by

William E. Moritz

SUDAAR No. 373
May 1969

This work was carried out at the Ames Research Center of NASA with the support of NASA Grant NGR 05-020-223 and with the aid of a NASA Traineeship. The material from SUDAAR No. 343 has been included here for the sake of completeness.

ACKNOWLEDGEMENTS

I would like to thank my adviser, Professor Max Anliker, for suggesting the problem studied in this dissertation and for his most helpful guidance and suggestions during the course of this research. Many other people have also contributed their time and effort in my behalf - notably past and present members of the Stanford-Ames Biomechanics Research Group. Dr. Eric Ogden of the Environmental Biology Division at NASA Ames has contributed helpful criticism and suggestions. Mr. Leonard Chan has been of great assistance in the laboratory. Professors I-Dee Chang and Leo Sapirstein have read the preliminary manuscript.

To my wife, Judy, I owe a special thanks for her patience and understanding.

This work was carried out at the Ames Research Center of NASA with the support of NASA Grant NGR 05-020-223 and with the aid of a NASA Traineeship.

ABSTRACT

For many years there has been a great deal of interest in evaluating the mechanical properties of arteries from studies on the propagation characteristics of the natural pressure wave induced by the heart. Relatively simple mathematical models for the mechanical behavior of the vessel wall were used in the analysis of data obtained in these studies. Recently, more elaborate models have been proposed which predict the transmission of not only pressure or distension waves but also torsion and axial waves. Measurements of the transmission characteristics of one type of wave allow for only a partial validation of the mathematical model since the mechanical properties of the wall and their frequency dependence are unknown. A technique to generate all three types of waves and monitor their transmission characteristics, speed and damping, was therefor devised.

The transmission characteristics of artificially induced pressure, torsion and axial waves were determined in the exposed carotid artery of 6 dogs while at least one of the three types of waves was studied in 25 other dogs. The animals were mature male mongrels of unknown age, weighing between 20 and 40 kg. They were anesthetized with 30 mg/kg i.v. sodium pentobarbital (Nembutal) and were kept in the supine position throughout the experiments.

Complex Fourier analysis and the interference of wave reflections were eliminated by the use of small amplitude, finite trains of sine waves. These were generated by a split-ring collar device placed around the vessel and attached to two electromagnetic shakers. One of these generated simultaneously pressure and axial waves while the other induced torsion waves. The peak-to-peak amplitudes of the pressure waves were less than 10 mm Hg and those of the torsion and axial waves were less than 2 mm. The frequency range covered was 20-100 Hz with some data on pressure and axial waves taken in the range 20-200 Hz.

The induced wall displacements were monitored with the aid of a pair of electro-optical tracking units equipped with a lens system that allowed for a resolution of 2×10^{-4} cm. These devices were able to follow the motion of small paper targets attached to the vessel at two points

a known distance apart. Small (1 mm diameter) catheter tip capacitance pressure transducers originally designed for wind-tunnel model studies were used to study the transmission of the pressure waves. The outputs from the pressure transducers and optical trackers were recorded on an oscillograph.

Wave transmission data was also acquired on the effect of varying the arterial pressure, the initial stretch and the surrounding medium of the vessel together with the signal amplitude on the transmission characteristics of each wave. In addition, the radius to wall thickness and initial stretch of the vessels were recorded in each experiment and averaged 8.5 and .41 repectively. The speed of the natural pressure wave in the carotid artery together with the naturally occurring wall motion was also measured.

The results indicate that the artificial pressure wave is non-dispersive with a speed of about 11 m/sec while the torsion and axial waves are mildly dispersive with speeds of 15-24 and 25-35 m/sec, respectively, for frequencies from 20 to 100 Hz. Theoretical results based on an isotropic model of the vessel wall predict that with the speed of the pressure wave given above the torsion and axial waves should travel about twice as fast as was found in these experiments. This discrepency may be interpreted as an indication of an anisotropic wall behavior. Specifically, the vessel appears to be approximately twice as extensible in the axial as in the circumferential direction.

The attenuation of all three types of waves follows an exponential pattern of the form $A/A_0 = \exp(-k\ \Delta x/\lambda)$ where k is the logarithmic decrement and $\Delta x/\lambda$ is the distance traveled in wavelengths. The values for k are independent of frequency and are of the order of 1.0 for pressure waves and 4-5 for axial and torsion waves. This high damping appears to be the result of the viscoelastic properties of the vessel wall.

TABLE OF CONTENTS

INTRODUCTION--Background Information and Motivation 1

CHAPTER I. THEORETICAL STUDIES 4

CHAPTER II. PREVIOUS EXPERIMENTAL INVESTIGATIONS 9

CHAPTER III. GENERAL EXPERIMENTAL PROCEDURE 12

CHAPTER IV. DATA REDUCTION AND ERRORS 28

CHAPTER V. RESULTS AND DISCUSSION 32

A. Natural Pulse Wave Speed and Natural Wall Displacements 33

B. Dispersion and Attenuation in Exposed Vessels 37

C. Transmural Pressure Effects on the Transmission Characteristics 51

D. Effect of Varying Amplitude 58

E. Effect of Varying Initial Stretch 62

F. Effect of Surrounding Medium 73

CHAPTER VI. SUMMARY AND CONCLUSIONS. 81

REFERENCES. 84

INTRODUCTION

Background Information and Motivation

Medical researchers have long been interested in the elastic behavior of blood vessels. This interest can be attributed to a variety of ailments and, in general terms, to the vital role that the proper elastic behavior of blood vessels plays in maintaining and regulating circulation. Besides this, the question of astronauts surviving space flights involving weightlessness for months or years and high decelerations during reentry has provided an additional incentive. It is expected that the cardiovascular system of man will adapt itself so well to the weightless state that it can no longer cope with reentry conditions after a long space flight unless an exercise or conditioning program is devised for the astronauts. We know from experience that after prolonged bed rest--which can be interpreted as a partial simulation of weightlessness--the cardiovascular system shows signs of deconditioning. This manifests itself by a reduced tilt-table tolerance or by orthostatic hypotension and syncope, which is attributed to an excessive diminution of the cardiac output caused by the pooling of blood in the lower parts of the body. This pooling is due to a reduced ability of the veins to resist the higher transmural pressures induced by the hydrostatic head.

It appears that the prolonged absence of normal stimuli such as the variation of the hydrostatic pressure with posture could cause the walls of blood vessels to become more elastic. Since gravity-induced stimuli are absent during zero-G flight, we must expect a loss of the ability of the vessels to resist deformation at higher pressures, which theoretically could prove fatal during reentry conditions. To prevent this, we have to devise not only an exercise or conditioning program for astronauts, but also reliable methods of measuring changes in the elastic behavior of blood vessels. Such methods could then be used to determine the effectiveness of an exercise or conditioning program during a prolonged space flight. Besides this, they might lend themselves to various clinical applications and possibly to the early detection of atherosclerosis.

Ideally, the measurement of the distensiblity and elastic properties of blood vessels should not require a penetration of the skin. A

nontraumatic method could for example be based on the fact that certain characteristic features associated with the generation and transmission of sound or pulse waves in a given medium can be related to the elastic properties of that medium. It has long been known that the speed of a pressure pulse in a blood vessel is an approximate measure of the elastic behavior of the vessel. In view of the fact that the elastic behavior can change quite rapidly with time and varies with size, location and nature of the vessel, a method based on wave generation and transmission would be particularly appropriate since it yields essentially local and instantaneous values. In the case of arteries we could utilize the natural pulse wave generated by the heart as has been done for more than a century, while for veins we would have to generate an artifical pressure wave. The effective Young's modulus, E, could then be estimated with the aid of the Moens-Korteweg equation

$$V^2 = \frac{Eh}{2\rho_f a}$$

if the wave speed V, the radius of the vessel a, the wall thickness h and the blood density ρ_f are known. Estimates for E obtained in this manner from a single wave speed measurement can, however, not be expected to be sufficiently accurate to reflect reliably changes in the effective Young's modulus of the vessel wall. The Moens-Korteweg equation is based on an extremely simple mathematical model for the mechanical behavior of blood vessels and their surroundings. While most noninvasive techniques currently available will only measure the wave speed V, the application of a pulsed laser doppler flow meter may provide the ability to monitor also the wall thickness and diameter of the vessel nontraumatically.

A more precise quantitative description of the wave transmission characteristics in terms of the physical and geometric properties of the blood vessels is obviously needed. As will be shown in Chapter I, the vessel can transmit basically three types of waves--a distension or pressure wave, a torsion wave and an axial wave. The transmission characteristics of each wave depends on the elastic or viscoelastic properties of the vessel wall along with a number of other parameters (also to be mentioned in Chapter I). If the vessel wall happens to be nonistropic, then measurements made on only one type of wave would provide insufficient

information from which to deduce the true viscoelastic properties of the vessel. It thus becomes necessary to study the dispersion and attenuation of the three types of waves mentioned above in a particular vessel under various conditions in order to check the validity of any mathematical model used to deduce the mechanical behavior of blood vessels.

To this end a series of experiments have been conducted to measure both the phase velocity as a function of frequency (dispersion) and the attenuation of pressure, torsion and axial waves in the carotid artery of anesthetized dogs. In addition to studying the transmission characteristics of each wave in the exposed artery, studies were also made to determine: a) the speed of the natural pressure wave and the magnitude of any naturally occurring wall motions, b) the effect of changing the transmural pressure levels in the artery on the transmission characteristics of the vessel wall, c) the linearity of the mechanical behavior of the vessel wall by changing the amplitude of the three types of waves, d) the effect of changes in the initial stretch of the vessel and e) the effect of the surrounding medium on the dispersion and attenuation of each wave.

The carotid artery was selected because of its favorable geometry and ease of accessibility.

I. THEORETICAL STUDIES

Considerable effort has already been made to predict the transmission characteristics of sinusoidal pressure waves in blood vessels by utilizing various kinds of mathematical models for the mechanical behavior of arteries and veins. Significant theoretical contributions are attributed to Witzig (1), Iberall (2), Morgan and Kiely (3), Womersley (4), Hardung (5), Klip (6) and other investigators. Reviews of theoretical as well as experimental studies of waves in blood vessels and the mechanical behavior of arteries and veins in general have been made by McDonald (7), Fox and Saibel (8), Rudinger (9), Skalak (10) and Fung (11).

From recent theoretical studies (12,13) we know that blood vessels can transmit three different types of waves if they behave like fluid-filled circular cylindrical shells. In these studies the waves are characterized by their mode shapes which are defined in terms of the displacement components u,v,w of an arbitrary point of the middle surface of the shell as illustrated in Figure 1. The waves are distinguished by the dominant displacement component at high frequencies. Accordingly we denote them as axial, torsion and distension waves. Each of these three types of waves has distinctly different transmission properties. Moreover, these properties depend strongly on whether the mode shapes are axially symmetric. When we restrict ourselves to axisymmetric waves, the results of a parametric study made in references (12) and (13) reveal the following characteristic features of the three types of waves. The distension waves are only mildly dispersive and have a relatively low speed for either the elastic or viscoelatic case. They are associated with strong intraluminal pressure fluctuations and are therefore also referred to as pressure waves. The torsion waves are nondispersive for elastic vessels and mildly dispersive for viscoelastic shells. They are somewhat faster than the pressure waves and theoretically do not produce any pressure perturbations for axisymmetric modes if the fluid is inviscid. Finally, for both elastic and viscoelastic walls, the axial waves also exhibit relatively mild dispersion and have the highest speeds. When the fluid can be considered as inviscid they exhibit only minute pressure fluctuations.

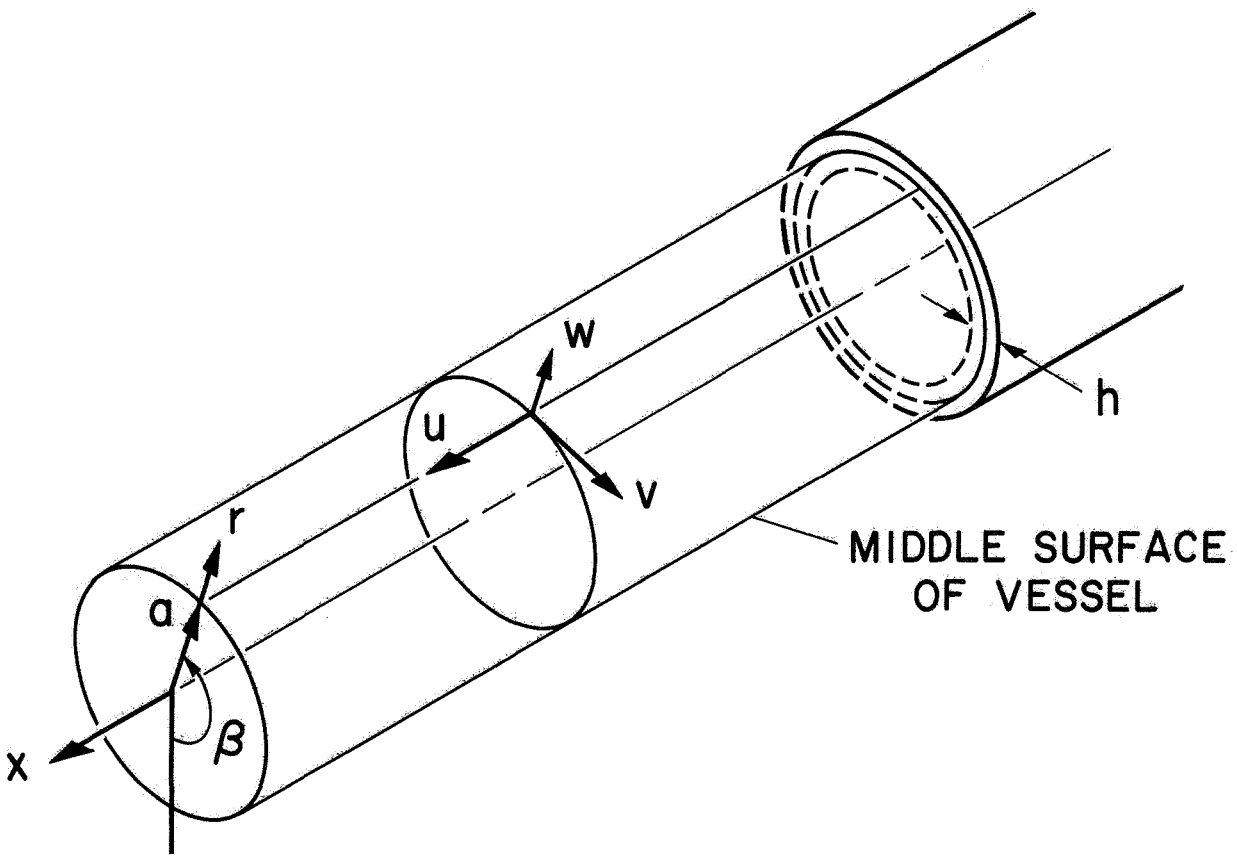

Figure 1. Coordinate system and displacement components u, v, w of an arbitrary point of the middle surface of circular cylindrical shell model for arteries.

Jones et al (14) have studied from a theoretical standpoint the effect of blood viscosity and external constraints on the transmission characteristics of pressure and axial waves. Their results indicate that for frequencies in the range 20-200 Hz the effect of blood viscosity on the speed of the pressure wave is minimal while a slight rise in the speed of the axial wave with increasing frequency is predicted as a result of viscosity. They have also predicted that blood viscosity will have little effect on the damping of the two types of waves at high frequencies.

Meanwhile, Wells (15) assumed an orthotropic, elastic shell model for the vessel wall and carried out an analysis similar to that of Anliker and Maxwell (12) to predict the transmission characteristics of the three types of waves.

The relevance of these theoretical findings depends, of course, on the validity of the mathematical model that was introduced in the analysis for the mechanical behavior of the blood vessels. Of particular significance in the prediction of the wave transmission characteristics are the constitutive laws obeyed by the vessel wall. For instance, in reference (13) the wall was assumed to be isotropically and linearly viscoelastic, incompressibile and behaving like a Voigt solid in shear. Since the wall properties are unknown, they are considered as free parameters in the mathematical model and are to be determined from experimental wave transmission data. The viscoelastic properties can for example be evaluated by measuring the propagation characteristics of one type of wave. Knowing these parameters we can then predict the dispersion and attenuation of the other two types of waves and by comparing them with the transmission data obtained for such waves we can examine the overall validity of the mathematical model. By proceeding in this manner it should in particular be possible to assess the assumptions made regarding the viscoelastic and isotropic behavior of the wall.

There are a number of properties and parameters which may effect the transmission of the various types of waves. They may be summarized as:

1. Elastic properties of the vessel wall
2. Diameter and geometry of the vessel wall
3. Thickness of the vessel wall

4. Density of the vessel wall
5. Density of the blood
6. Viscous properties of the vessel wall
7. Compressibility of the blood
8. Viscosity of the blood
9. Transmural pressure
10. Nature of the wave being transmitted
11. Longitudinal stretch of the vessel
12. Mean flow and nature of the flow
13. The surrounding medium of the vessel.

Items 1-8 above are generally beyond our control and thus cannot be varied in a systematic manner. Items 9-13, however, can be varied to some extent in an effort to determine changes in the transmission characteristics of the various types of waves in response to these varied parameters. Maxwell and Anliker (13) have carried out a parametric analysis in which they have varied the transmural pressure and the initial stretch (i.e. tension) of the vessel along with variations in such parameters as wall thickness to radius ratio and wall viscosity. Their purpose was to establish, theoretically, the effect of parametric changes on the dispersion and attenuation of the three types of waves.

Since the physical dimensions of the vessel as well as its initial stretch may effect its transmission characteristics, data was taken on the radius and wall thickness of the vessel together with the in-vivo stretch present. The diameter and twice the wall thickness of the exposed, in-vivo artery were measured with the aid of a caliper and the data are given in Table I. Also shown in Table I are in-vivo strain values determined by noting the decrease in length of an arterial segment upon being excised and drained of blood.

TABLE I.

DATA ON DIAMETER, WALL THICKNESS AND IN-VIVO STRAIN OF LEFT CAROTID ARTERIES IN DOGS

Experiment	Weight (kg)	2a (mm)	2h (mm)	a/h	l (cm)	l_o (cm)	$\Delta l/l_o$
235	28.6	5.0	.8	6.2	7.7	5.8	.33
236	35.4	5.0	.5	10.0	*	*	*
240	27.2	4.5	.5	9.0	7.0	4.8	.25
272	25.0	4.0	.5	8.0	6.5	5.0	.30
276	38.0	4.5	.5	9.0	7.3	4.6	.59
280	21.4	5.0	.5	10.0	7.0	4.9	.30
285	18.6	4.0	.5	8.0	6.0	4.3	.39
290	34.5	4.5	.5	9.0	4.7	3.5	.34
295	24.6	4.0	.5	8.0	5.3	4.4	.21
297	30.0	5.0	.5	10.0	5.4	3.9	.38
302	31.4	*	*	*	7.4	6.0	.23
314	27.6	5.0	.5	10.0	10.7	6.5	.65
323	20.0	4.0	.5	8.0	4.0	3.0	.33
325	23.0	4.5	.5	9.0	6.3	3.8	.66
326	17.3	4.0	.5	8.0	5.8	4.2	.38
327	22.6	4.5	.5	9.0	5.9	4.0	.48
332	23.5	3.5	.5	7.0	4.9	3.1	.58
334	23.0	4.0	.5	8.0	7.0	4.6	.52
336	25.0	4.0	.5	8.0	8.3	6.0	.37
337	37.0	6.0	.7	9.0	5.2	3.5	.48
338	25.0	4.0	.5	8.0	*	*	*
339	24.5	4.3	.5	8.6	5.1	3.6	.41
347	21.0	4.0	.5	8.0	5.1	3.5	.46
348	26.8	4.0	.8	5.0	5.8	4.0	.45
349	28.6	4.2	.5	8.4	4.2	3.0	.40
352	36.0	5.0	.5	10.0	6.0	4.5	.33
353	39.0	4.0	.5	8.0	8.3	6.0	.38
354	23.0	4.0	.5	8.0	4.0	2.9	.38
356	30.0	4.5	.5	9.0	6.6	4.8	.37
361	30.0	5.0	.8	6.2	4.8	3.3	.45

2a = outside diameter at normal blood pressure
h = wall thickness, in-vivo
l = in-vivo length of the vessel segment
l_o = excised length of the vessel segment
*° indicates that no measurements were made

Average radius to wall thickness ratio (a/h) = 8.5
Average in-vivo strain ($\Delta l/l_o$) = .40

II. PREVIOUS EXPERIMENTAL INVESTIGATIONS

So far, most of the experimental wave transmission studies on blood vessels have dealt with the natural pulse wave generated by the heart. Particular efforts have been made to deduce information regarding the mechanical properties of arteries from the propagation characteristics of individual harmonic components of the natural pulse (7,16). The results obtained in this manner are based on the assumption that arteries behave like linear systems with respect to large amplitude pressure waves. When one considers that an average pressure pulse of 40 mm Hg can produce changes in the wall stress of the order of 10 percent of the effective Young's modulus, the assumption of linearity must be regarded with reservation. Indeed, recent investigations have provided new evidence for a nonlinear behavior of the vessel wall with respect to large amplitude pressure waves (17,18).

Rather than utilizing the natural pulse, some investigators (19,20, 21) have artifically induced transient pressure signals by means of an injection device or an electrically driven impactor. These signals were also of large amplitude and therefore linear analysis of them would be subject to the same criticism as that applied to the harmonic analysis of the pressure wave generated by the heart.

The propagation characteristics of waves in a given medium are usually described by the dispersion and attenuation of small harmonic signals, i.e. by the speed and decay of infinitely long sinusoidal waves as a function of frequency or wavelength. Since we in reality have signals of finite length and media of finite dimensions that may exhibit nonlinear phenomena, the determination of these properties can in some cases be encumbered by uncertainties and may generally require laborious computations. The uncertainties arise when the waves are not sufficiently small or conditions prevail that do not justify the assumption of a linear behavior of the system or when reflections modify the transient signals of interest. Extensive computations may have to be performed when the wave is of arbitrary shape since then the Fourier transform of the propagating signal has to be evaluated at various locations within the medium if its wave transmission characteristics are to be described in terms of the speed

and attenuation of harmonic waves as a function of frequency.

For a mildly dispersive medium, i.e. one in which the phase velocity varies by no more than a few percent whenever the frequency is changed by 10 percent, the need for Fourier transform computations can be circumvented if the transient signal is of the form of a finite train of sine waves. As shown in Figure 2, the Fourier spectrum of such waves is dominated by the frequency of the sine waves in increasing proportion to the length of the trains. Therefore, the speed of such a signal can be considered a good approximation of the phase velocity corresponding to the frequency of the sine waves. Also, it is possible to avoid the interference of reflections with the transient signal if the signals are sufficiently short in duration or if the medium exhibits strong attenuation. For sufficiently high frequencies and short trains the waves can be recorded before their reflections arrive at the recording site. In the case of strong attenuation, the reflections of a small wave may be completely damped out before they reach the transducer location.

This approach has been succesfully applied by Anliker et al (18) in a recent investigation of the dispersion and attenuation of pressure waves (distension waves) in the thoracic aorta of anesthetized dogs. The results of this study show that for frequencies between 40 and 200 Hz the aorta exhibits only mild dispersion but exhibits strong attenuation that can largely be attributed to dissipative mechanisms in the vessel wall. At normal blood pressure levels the wave speed during diastole can have a value between 4 and 6 m/sec. Moreover, for all frequencies considered, the amplitude ratio of propagating waves exhibits the same exponential decay pattern with distance measured in wavelengths.

These methods have also been applied to the study of wave transmission characteristics of pressure waves in the abdominal vena cava of anesthetized dogs by Anliker et al (22).

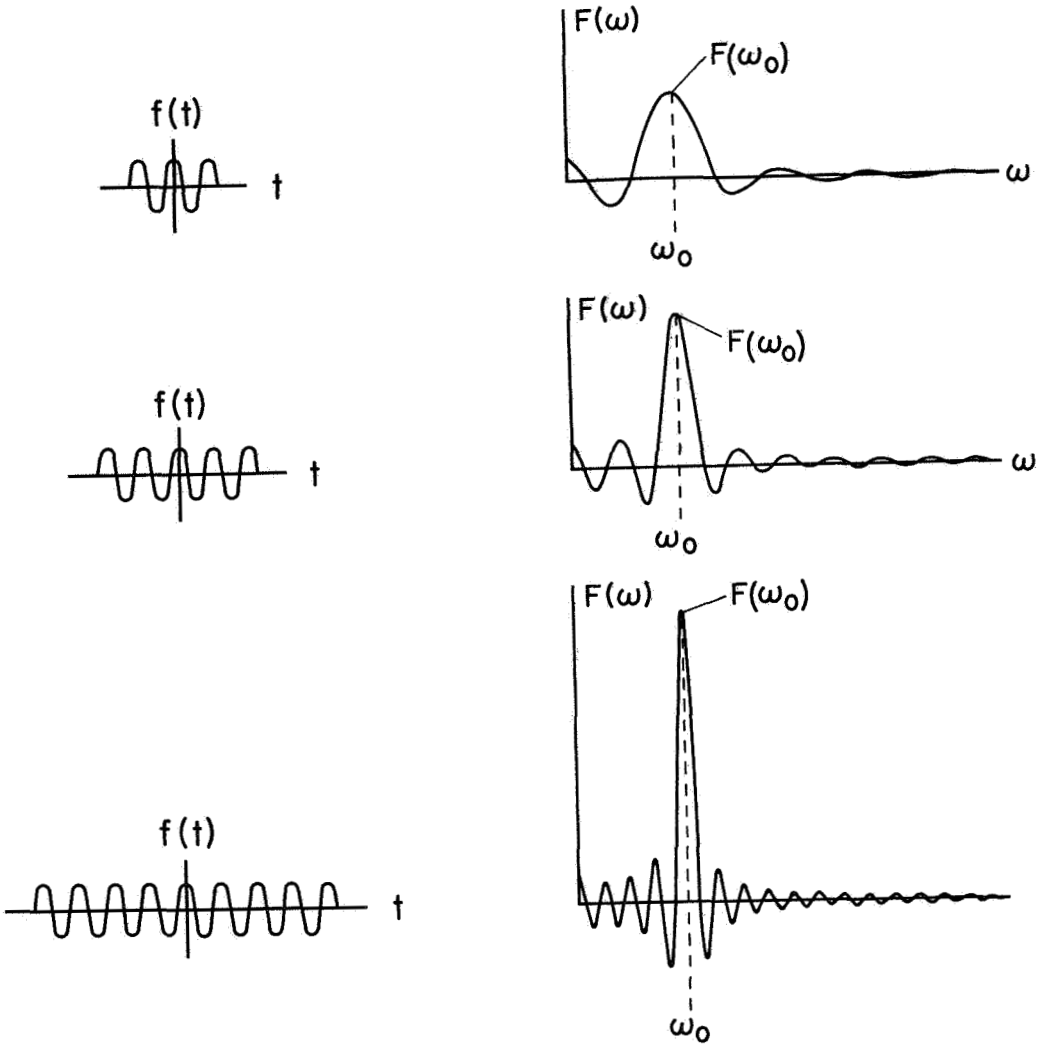

$$f(t) = \frac{1}{2\pi} \int_{-\infty}^{\infty} F(\omega)\, e^{i\omega t}\, d\omega \qquad F(\omega) = \int_{-\infty}^{\infty} f(t)\, e^{-i\omega t}\, dt$$

$$f(t) = \begin{cases} \cos(\omega_0 t), & |t| < \frac{\tau}{2} \\ 0, & (t) > \frac{\tau}{2} \end{cases} \qquad F(\omega) = \frac{\tau}{2} \left[\frac{\sin\left(\frac{\omega-\omega_0}{2}\right)\tau}{\left(\frac{\omega-\omega_0}{2}\right)\tau} + \frac{\sin\left(\frac{\omega+\omega_0}{2}\right)\tau}{\left(\frac{\omega+\omega_0}{2}\right)\tau} \right]$$

Figure 2. Fourier transform of finite trains of sine waves.

III. GENERAL EXPERIMENTAL PROCEDURE

To measure the dispersion and attenuation of the various types of waves, finite trains of sinusoidal axial and torsional displacements were induced in the walls of surgically exposed carotid arteries of anesthetized dogs. They weighed between 20 and 40 kg and were anesthetized with approximately 30 mg/kg i.v. sodium pentobarbital (Nembutal). Throughout the experiments the dogs were kept in the supine position.

The surgical exposure consisted of making a small incision in the clavicle region of the neck and exposing the right omocervical artery. This artery was cannulated with a flexible, radio-opaque catheter attached to a Statham P23Dd arterial pressure transducer. The tip of the catheter was positioned in the brachiocephalic artery at the root of the carotids with the aid of an X-ray fluoroscope. The blood pressure was monitored throughout the experiment as an indicator of the general physiological state of the animal and also an approximate measure of the blood pressure in the carotid arteries.

Next a midline incision approximately 20 cm long was made on the ventral side of the neck and the right and left sternomastoideus muscles were separated to expose the sternohyoideus muscle layer.

As shown in Figure 3, the common carotid arteries in the dog originate from the brachiocephalic artery and supply blood to the head and neck. Since the first branch of the carotid artery (cranial thyroid) is located 15 to 20 cm above the brachiocephalic we thus have an unusually long section of branch-free vessel of nearly constant geometry.

In each section in the chapter on Results and Discussion a detailed description of the particular surgical procedure used to study the various effects will be given. In general, the following procedure was used.

The muscle layers surrounding the carotid artery were stripped away to expose the vessel over a distance of 10-15 cm. In addition, the vagus nerve and carotid sheath were separated from the vessel over its exposed length.

The transmission of the pressure waves was determined by one of two methods. The needles from two pressure transducers of the type shown in Figure 4 were inserted into the lumen at two points 3.5 and 8 cm apart

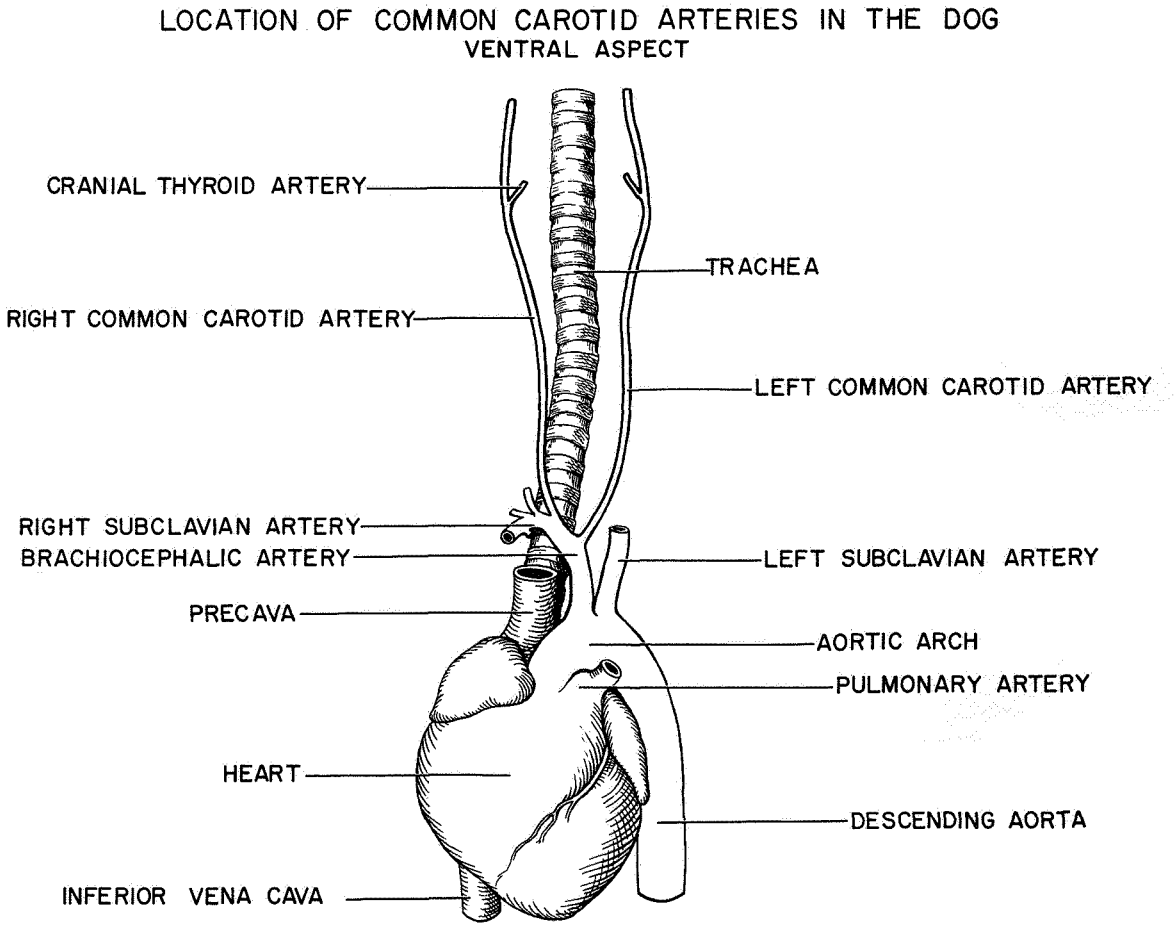

Figure 3. Pertinent anatomy of the neck region of the dog showing the location of the carotid artery with respect to the trachea and heart.

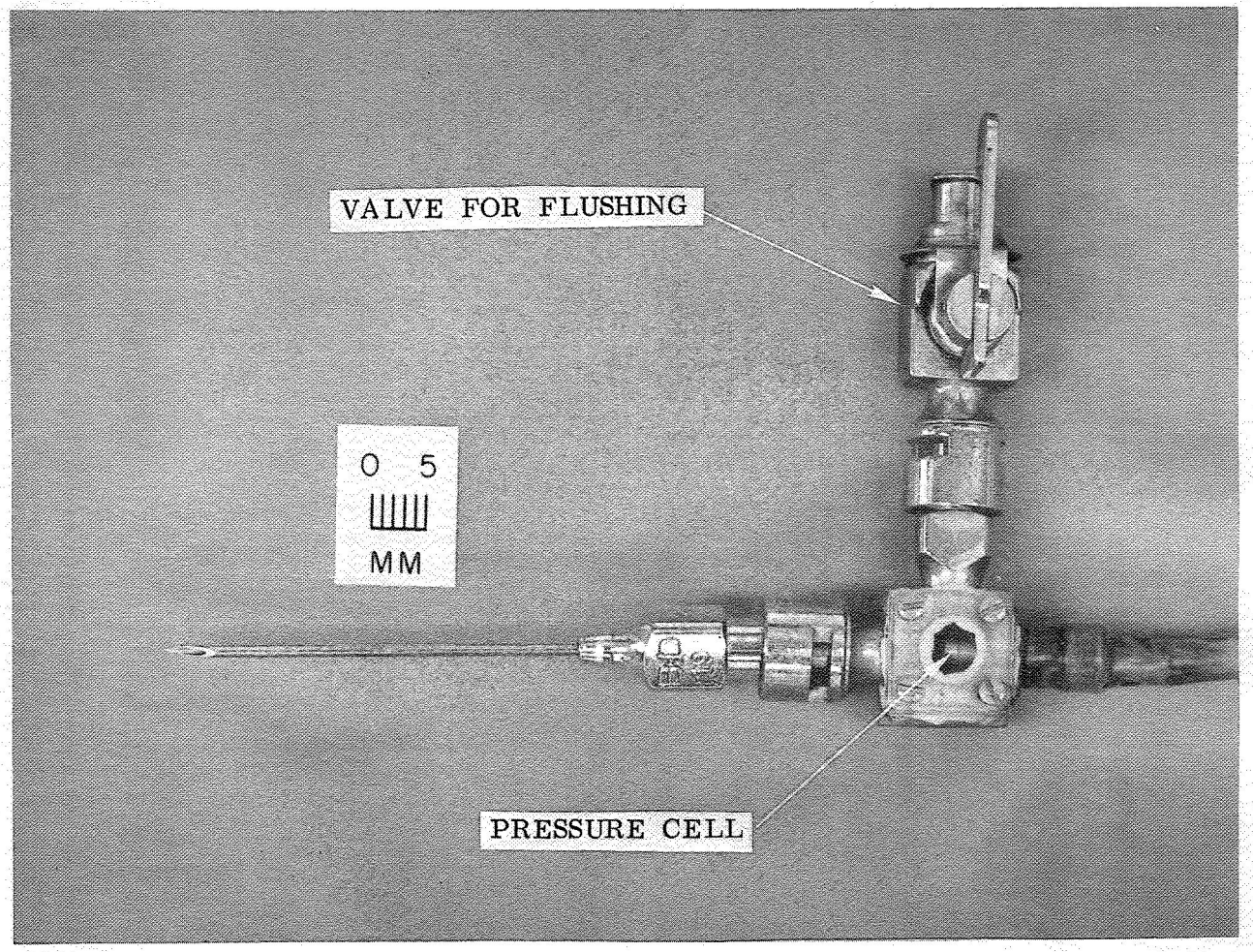

Figure 4. Pressure transducer consisting of Bytrex pressure cells HFD-5 built into a modified 3-way stopcock with needle attached.

and the local pressure fluctuations as a function of time were recorded. The distance between the needle tips was determined to an accuracy of .1 cm by making use of the X-ray fluoroscope equipped with an image intensifier and a radio-opaque grid with a mesh size of 1 cm. As pressure transducers we used comercially available Bytrex pressure cells model HFD-5 that were imbedded in modified standard 3-way stopcocks. This arrangement provided for the easy attachment of various size needles and for flushing the chamber and needle during the course of the experiment. The Bytrex pressure cell has a fundamental frequency of 60 KHz in air and is linear within 1 percent from 0 to 300 mm Hg. The output from the bridge circuit was amplified by means of an Astrodata Model 885 DC amplifier.

In some experiments the pressure fluctuations were monitored with the aid of highly sensitive catheter tip capacitance pressure transducers originally designed for wind tunnel model studies and adapted for physiological applications. The transducers used had a diameter of 1 mm and were mounted on a flexible catheter that encloses the electrical leads and a venting tube (Figure 5). The cells form part of a capacitance bridge and the signals are recorded after amplification by a 100 KHz carrier amplifier. Their fundamental frequency is 82 KHz in air and they have a resolution of about .2 mm Hg and are linear within 1 percent from 0 to 200 mm Hg.

The catheter-tip manometers were inserted through two branches of the cranial thyroid artery. The transducers were positioned and the distance between them measured with the X-ray fluoroscope.

To monitor the axial and torsional wall displacements small target collars weighing less than .5 gm (Figure 6) were attached to the vessel 3 to 11 cm apart. They consisted of 2-4 mm sections of plastic tubing provided with a slit and silk threads to secure the target to the carotid artery. To limit the constriction to less than 15 percent of its diameter various collars of different internal diameters were available. Paper targets as shown in Figure 6 with a line of contrast in two perpendicular directions were then glued into place on each of the collars.

The motion of the targets in the axial and circumferential (torsion) directions was monitored with the aid of a pair of PhyisTech Model 39A electro-optical tracking units with lens configurations allowing for a resolution of 2×10^{-4} cm and a frequency response in excess of 2000 Hz.

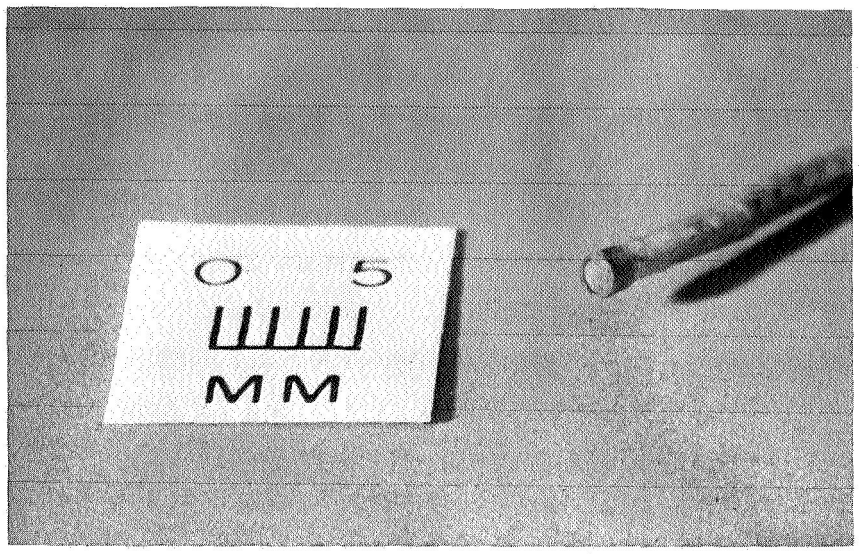

Figure 5. Capacitance type pressure transducer mounted on a flexible catheter for physiological applications. Diameter = 1.0 mm. Resolution approximately .2 mm Hg.

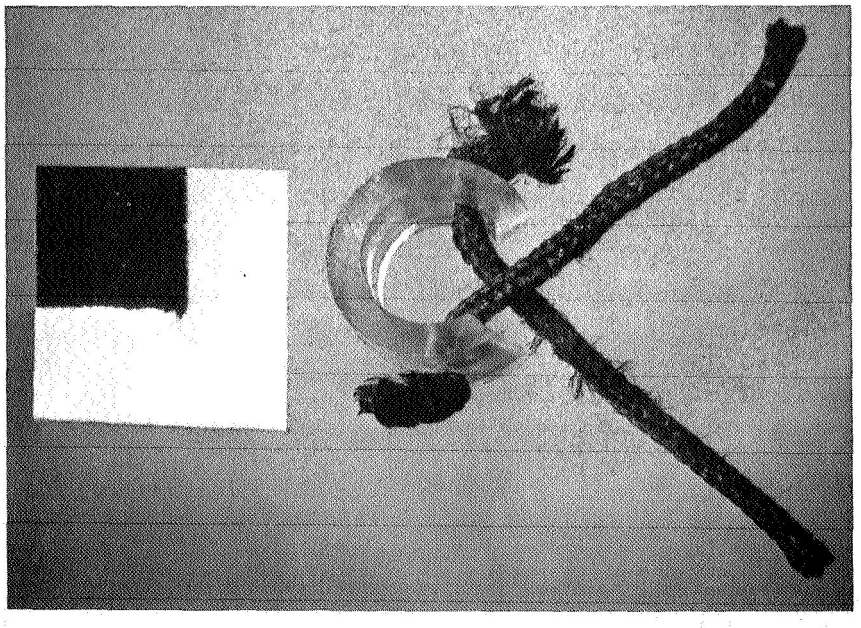

Figure 6. Plastic tubing used as target collar with threads to secure it to the vessel. Paper target shown was glued to the collar. Weight of target and collar is less than .5 gm.

Target illumination was provided by a quartz iodine light powered by a DC source.

The optical tracking system is designed to measure the motion of a line of contrast (i.e. a black-white interface) perpendicular to the optical axis. Light being reflected from the target is focused on a photo-emissive surface by means of the lens system as shown in Figure 7 below. The beam of electrons thus produced is then accelerated down the tube toward a small aperature in front of a photomultiplier tube. Simultaneously, current is applied to coils along the axis of the tube to cause the beam of electrons to be swept across the aperture. The output from the photo-multipier tube then shows a sharp jump (either increasing or decreasing depending on the orientation of the target) when the electronic image of the line of contrast passes the aperture. The point during the sweep at which the current from the PMT changes is then read out of the instrument and gives the position of the black-white interface during that sweep. The scanning rate is 50KHz and the field of view, resolution and working distance are determined by the particular lens system employed.

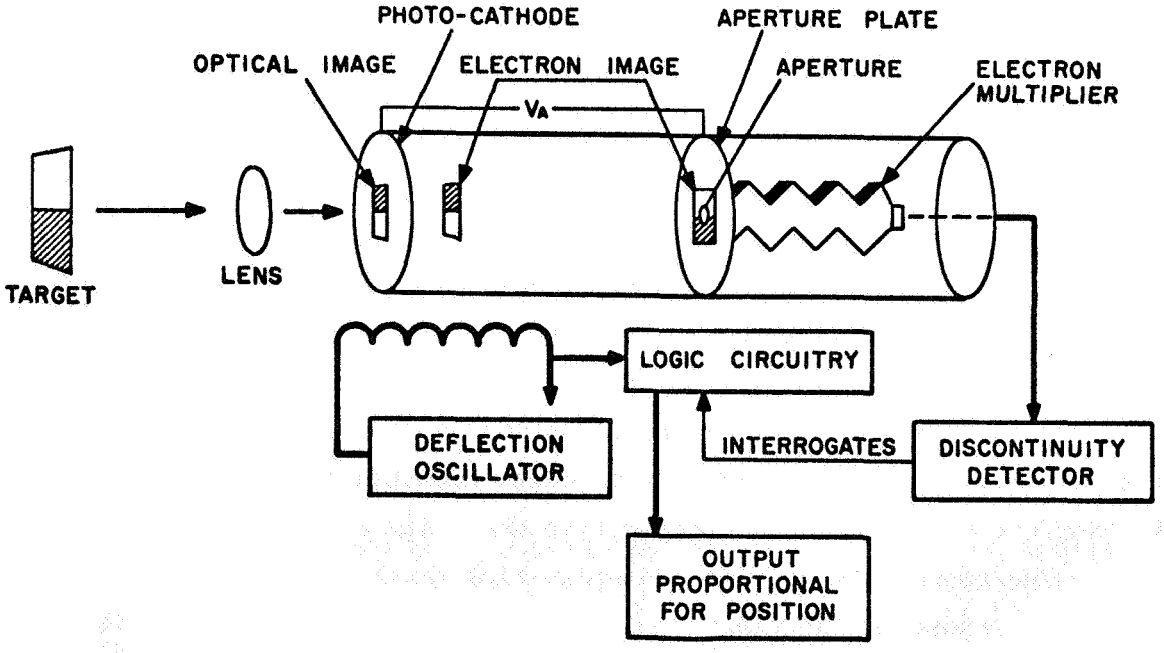

Figure 7. Principle of operation of the PhyisTech Model 39A electro-optical tracking system. V_A is the accelerating voltage.

Two sets of perpendicular coils in the optical head allow for the monitoring in two orthogonal directions either simultaneously (biaxial) or separately without reorienting the optical head. Front panel controls allow for selection of the tracking mode (horizontal, vertical or biaxial) desired, adjustment for various lighting conditions and for zero and gain control of the output amplifier.

The signals from the pressure transducers, including the Statham, and the optical trackers were recorded on a Honeywell Visicorder with galvonometers whose frequency response is flat up to 2000 Hz and paper speeds up to 2 m/sec. The Statham transducer, pressure cells and the optical tracking units including all amplifiers and recording devices were calibrated for each experiment.

The generation of pressure and axial waves was accomplished with the aid of two similar devices. The first consisted of the plastic collar shown in Figure 8. It was attached to the vessel 2 to 4 cm from the first target or transducer and connected to an electromagnetic shaker. Again, various sizes were available to adapt to the individual artery. The collar-artery interface was padded with short pieces of braided umbilical tape to insure good mechanical coupling. In all cases the constriction of the vessel was less than 15 percent of the diameter. An annular piston was thus formed by the constriction which allowed for the simultaneous generation of axial and pressure waves.

The second device is shown in Figure 9. It allows not only for the generation of pressure waves and axial wall displacements but can generate torsional wall motions as well. Its attachment to the vessel is by means of a stainless steel split-ring with a 4 mm internal diameter. After being padded with umbilical tape and placed around the artery the ring is inserted into a connecting fitting made of anodized aluminum and providing a bearing surface so that the ring may rotate about the axis of the vessel.

The connecting fitting and split-ring assembly serve essentially the same purpose as the plastic collar device mentioned above. This assembly is then attached to the electromagnetic shakers described below.

The split-ring is connected, by means of the cross-link shown in Figure 9 and another rod not shown in the figure, to an electromagnetic shaker. These rods transmit the sinusoidal motion of the shaker to the

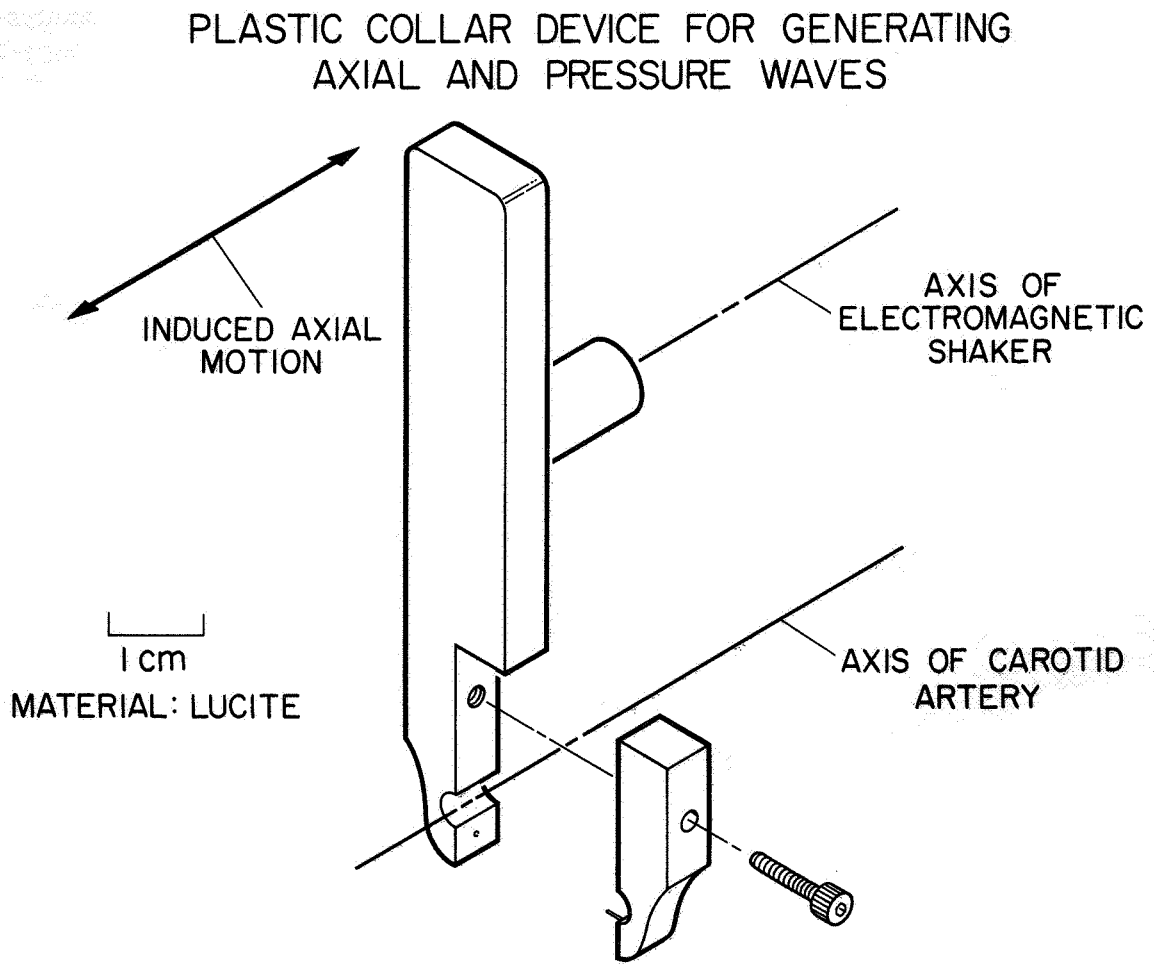

Figure 8. Schematic diagram of plastic collar device used to generate axial and pressure waves.

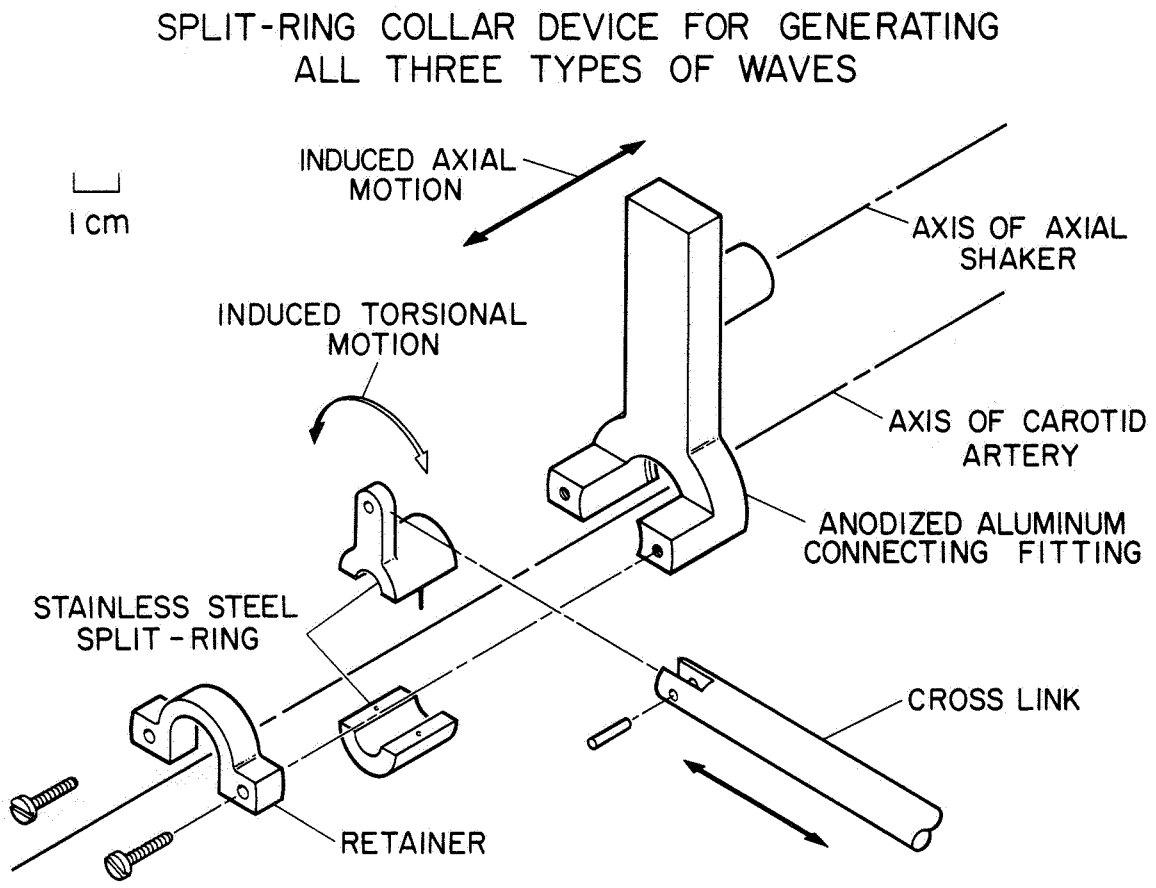

Figure 9. Schematic diagram of device used to generate pressure, torsion and axial waves. Note that another rod not shown in this figure attaches to the right hand end of the cross-link (See Figure 11). This rod is connected to an electromagnetic shaker and transfers the sinusoidal output of the shaker to the cross-link.

split-ring and cause the vessel to rotate in a sinusoidal manner about its axis. The motion of the cross-link (Figure 9) was monitored with the optical trackers and was found to be very close to sinusoidal for the frequency range of interest.

The optical tracking units have the capability of monitoring, simultaneously, motion in two orthogonal directions perpendicular to the optical axis. In theory then, it would be a simple matter to measure simultaneously the axial and torsional wall displacements. In practice, however, the difficulties encountered when trying to do this made data acquisition extremely difficult. When the optical trackers are used in the biaxial mode, the effective field of view is reduced and the alignment of the trackers becomes more critical. In addition, the design of the biaxial output amplifiers in the optical tracking system is such that controlling the gain and zero adjustments require partial dismantling of the control units.

Figure 10 shows the targets, plastic collar and shaker in place. The view seen by the optical trackers is shown in Figure 11. Figure 12 shows the torsion wave generator in place on the artery.

The electromagnetic shakers are shown in Figure 12 and 13. They consist of a solenoid whose core is connected to a lightweight piston. Each device is driven by a separate electronic oscillator and high fidelity amplifier which is gated by a tone burst generator. When the shaker is activated, axial or torsional wall displacements in the form of finite trains of sine waves are generated. The frequency and amplitude of these waves are controlled by the electronic oscillator while the number of sine waves contained in the trains and the intervals between successive trains are determined by the tone burst generator. The frequency range was from 20 to 200 Hz although most data was restricted to the range 20 to 100 Hz. The amplitude of the axial waves at the first station was always less than 2 mm peak-to-peak. The amplitude of the torsion waves was always less than 2 mm peak-to-peak and generally less than 1.5 mm. With a vessel whose outside diameter is 4 mm, a 1.5 mm circumferential motion is equivalent to a rotation of less than 45°. In most cases, an effort was made to restrict the rotation to less than 30° (or about 1 mm peak-to-peak wall displacement).

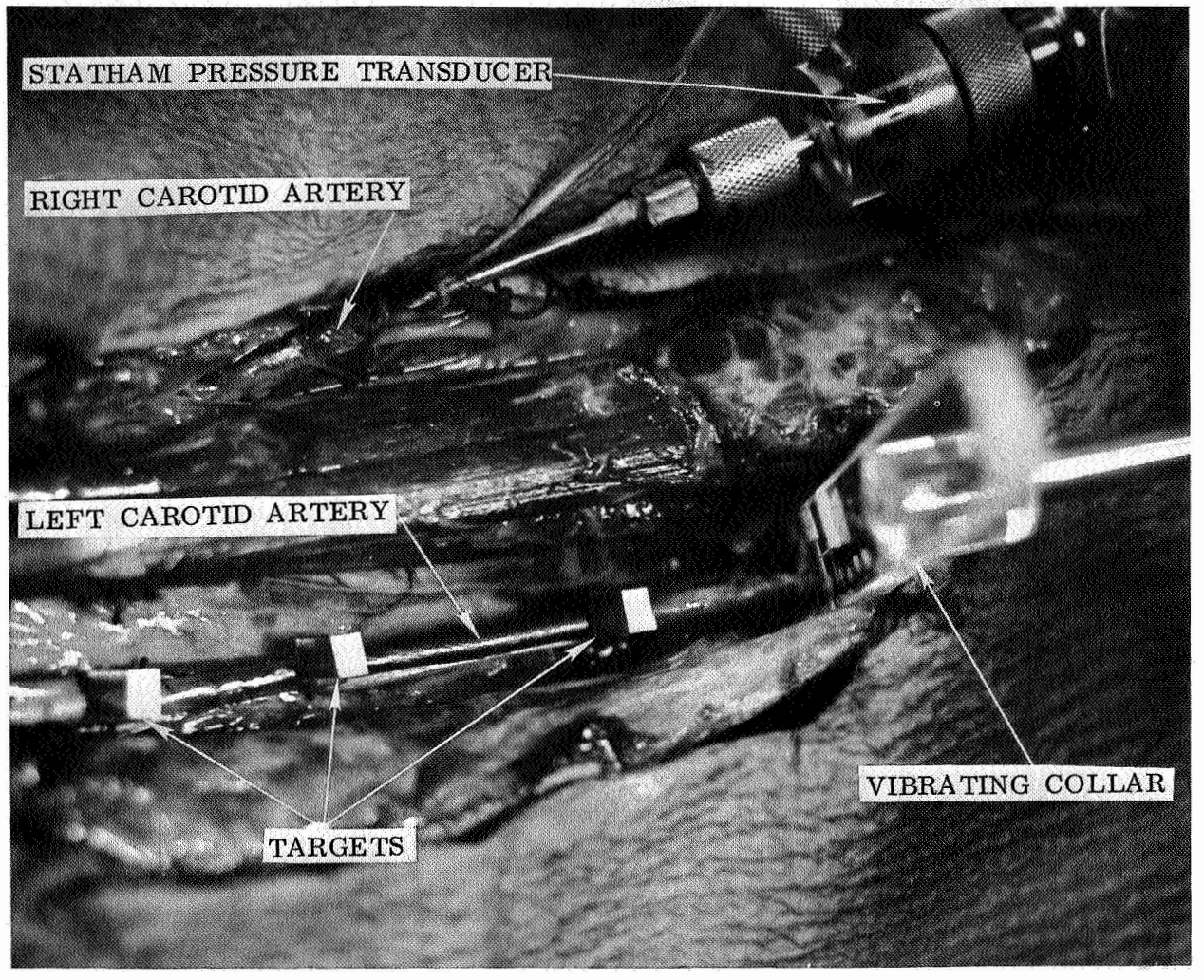

Figure 10. Surgically exposed carotid arteries. Targets and plastic vibrating collar are attached to the left carotid, a cannula from the Statham transducer is inserted into the right carotid in this experiment. The Statham was usually placed in the right omocervical artery. Three targets are shown in this picture.

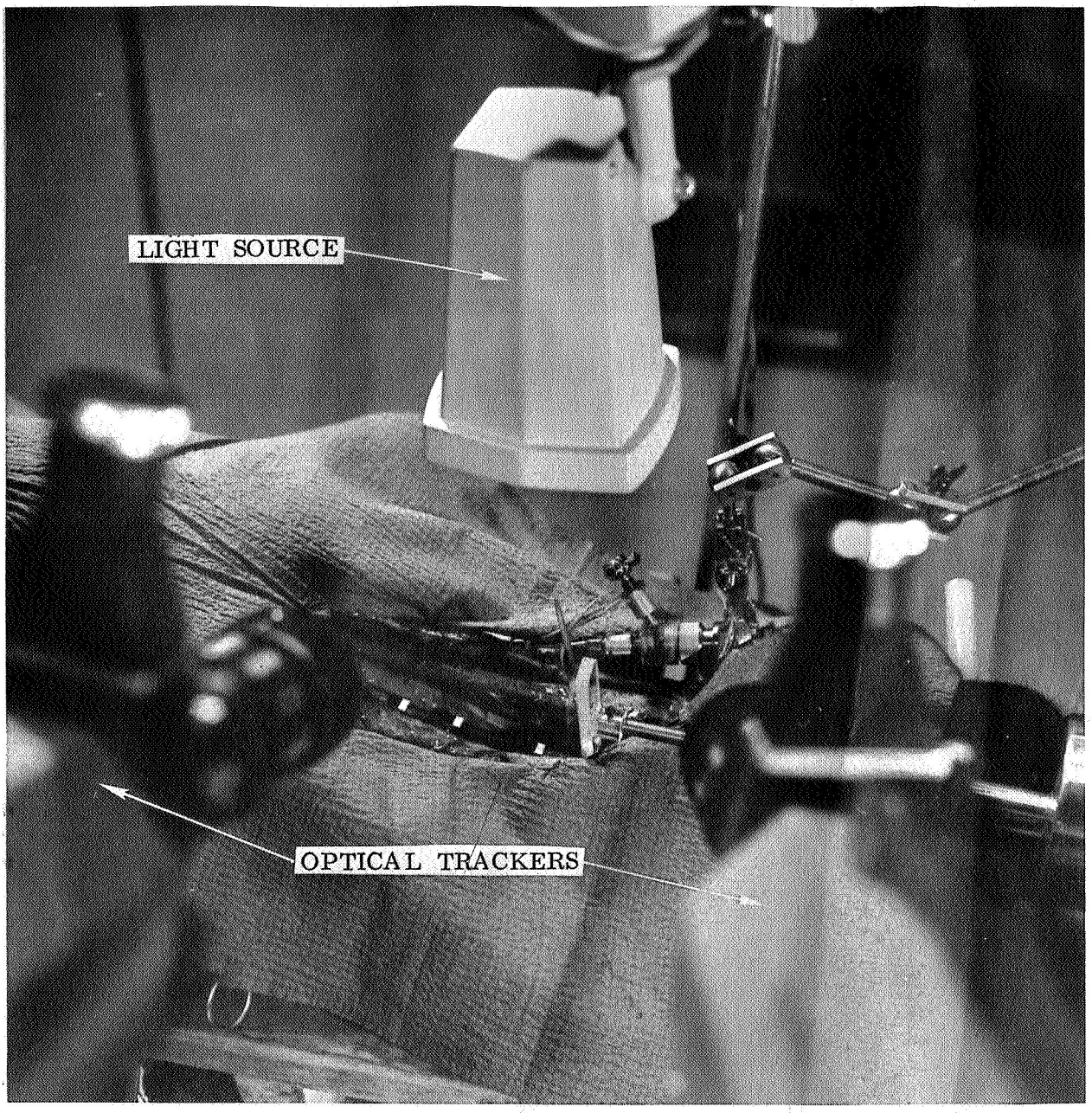

Figure 11. View of experimental arrangement with PhysiTech electro-optical trackers. Distance between the lenses and targets was approximately 33 cm.

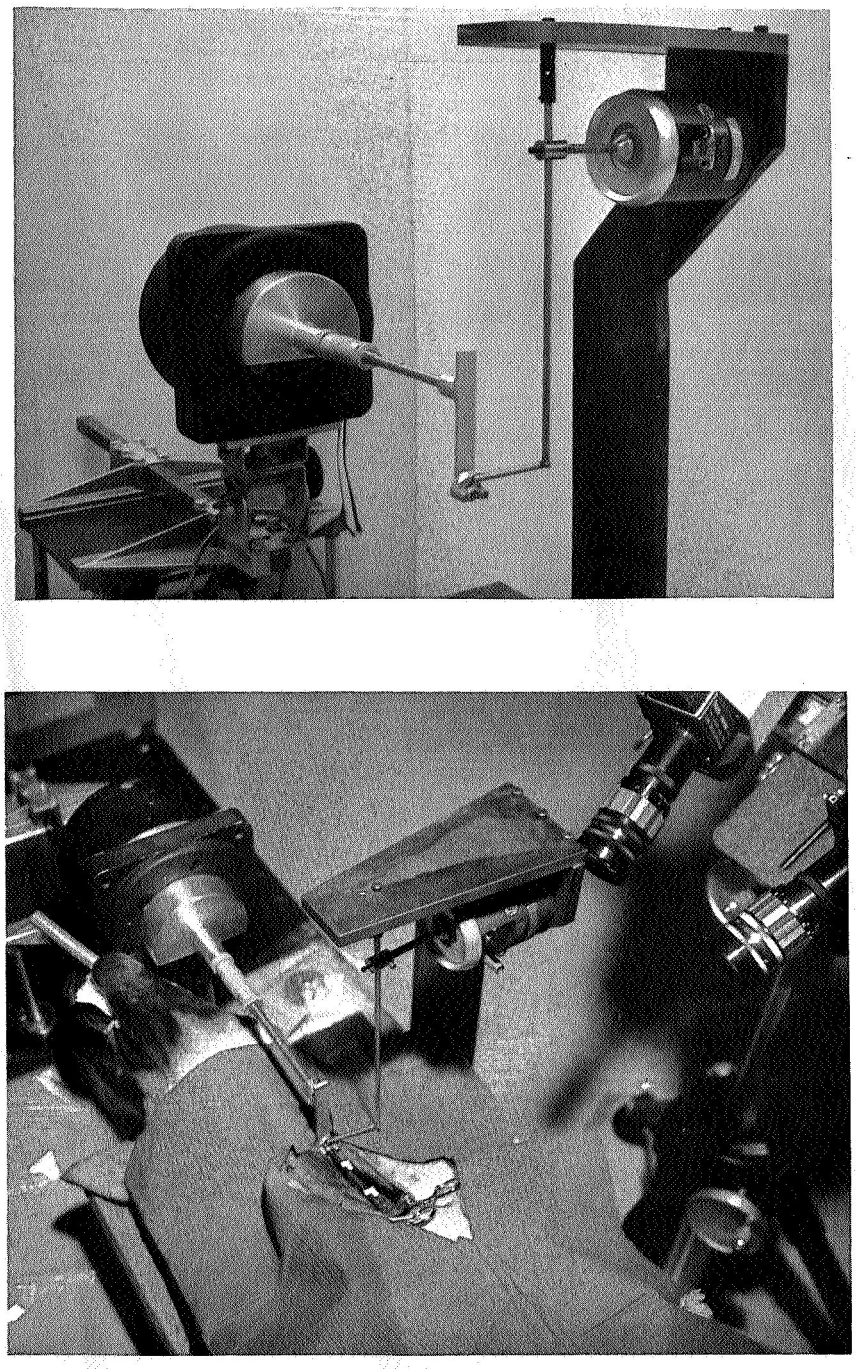

Figure 12. Top photograph shows the wave generator in Figure 9 attached to its two electromagnetic shakers. The bottom photograph shows the generator in place on the left carotid artery along with the targets and optical trackers.

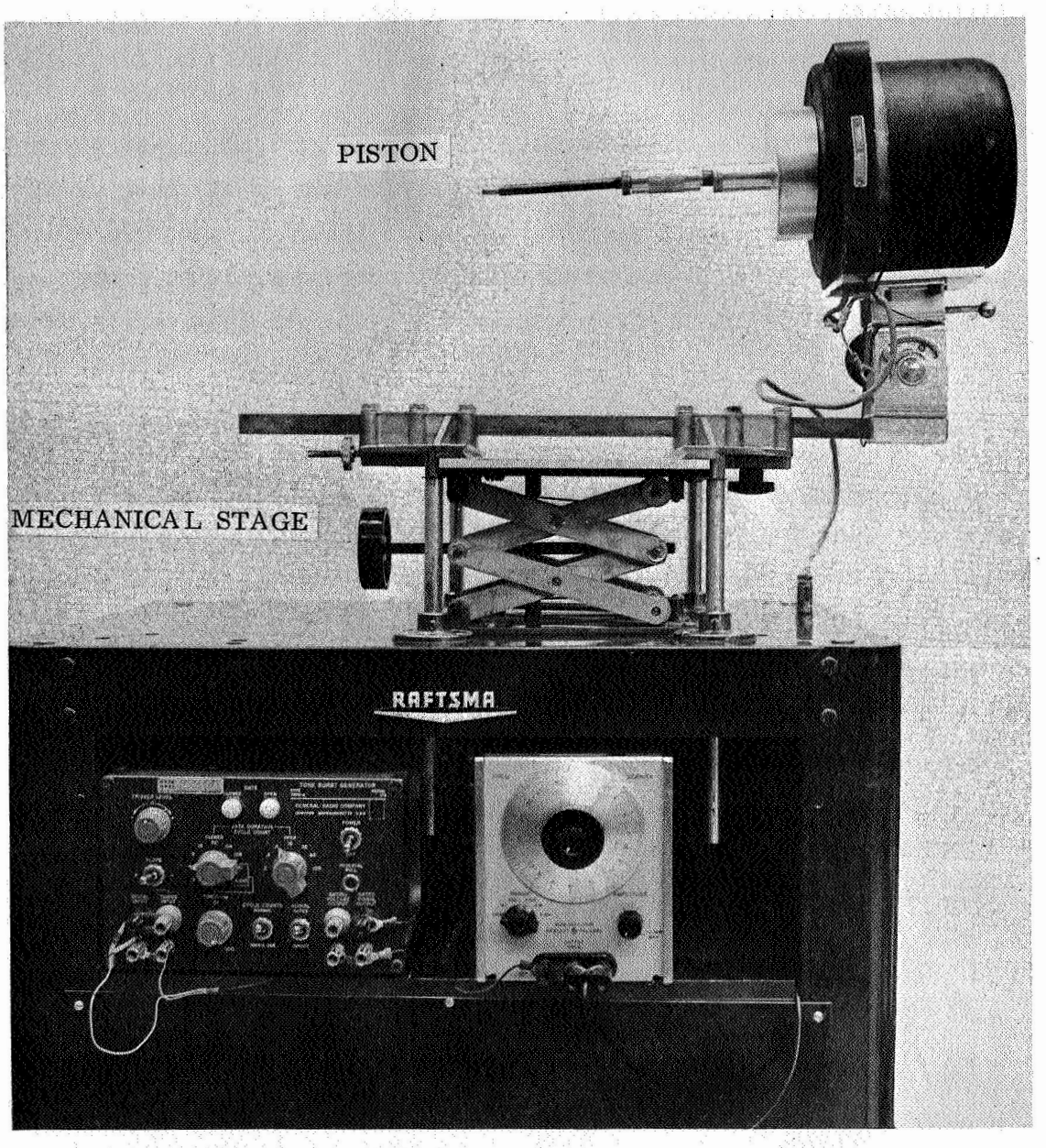

Figure 13. Electromagnetic shaker with electronic oscillator and tone burst generator. To generate axial wall motion the end of the piston is attached to the vibrating collar devices shown in Figures 7 and 8.

In attaching the plastic collar or split-ring assembly to the vessel the natural stretch of the vessel was left unchanged. Moreover, the piston of the axial shaker was carefully aligned with the axis of the vessel to minimize the possibility of generating non-axisymmetric waves in the carotid artery.

Theoretical considerations (12,13) predict that non-axisymmetric waves of all three types (distension, torsion and axial) have vastly different transmission characteristics than do their axisymmetric counterparts. On the basis of the model used in references (12,13), they exhibit strong dispersion and an attenuation per wavelength that varies strikingly with frequency and therefore would be easily recognized among axisymmetric signals. However, no evidence of their presence could be discerned from our recordings on any type of wave.

In some experiments the intraluminal pressure fluctuations at the external target locations were monitored together with the axial wall displacements. This was accomplished with the aid of the capacitance pressure cells mentioned above. A tracing of a representative recording of both types of waves is given in Figure 14. In most experiments the external targets were removed when taking data on the pressure waves so as to eliminate any interference between themselves and the pressure transducers.

With the transducers and targets in place, waves in the form of finite trains of sine waves were generated in the carotid artery and the speed and damping of these waves was measured.

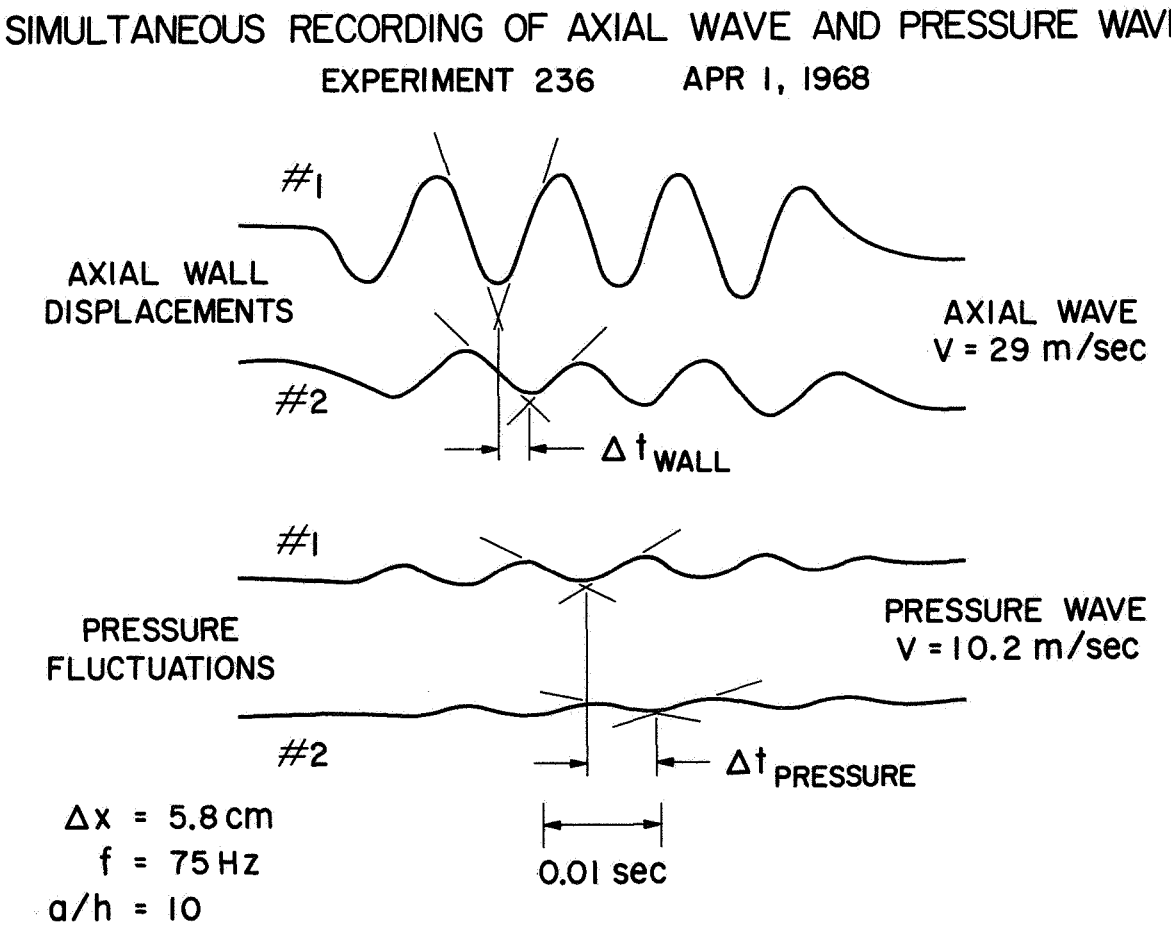

Figure 14. Tracings of simultaneous recordings of pressure- and axial waves in the left exposed carotid artery. Both types of waves were induced simultaneously by the vibrating collar. The pressure recordings were obtained with the aid of catheter-tip manometers of the kind shown in Figure 14. The manometers were located at the same cross-sections as the external targets by means of a fluoroscope. In this instance, the blood pressure was 205/170 mm Hg. Note the difference in transmission time for the two types of waves.

IV. DATA REDUCTION AND ERRORS

There are various ways in which the time of propagation of the natural pressure pulse wave can be defined and the resulting Δt may depend on that choice. For example, we may define it as the time of propagation over a distance Δx of a characteristic point of the wave front, say the point corresponding to 1/3 the pulse pressure, or we can choose, as shown in Figure 15, the intersection of the tangent in the inflection point of the wave front with a line approximating the terminal phase of the preceeding pulse. In this study, we consistently made use of the latter definition.

By contrast, the speed of the artifically induced trains of sine waves could be determined with far greater certainty. The mildly dispersive nature of the carotid artery with respect to small axisymmetric distension, torsion and axial waves and the absence of reflection interference made it possible to measure the speed of such signals virtually independently of the selection of the characteristic point. As illustrated in Figure 16, we have chosen as characteristic points the intersection of the tangents to the sine waves at two successive inflection points. At a recording speed of 1 m/sec or higher the time difference Δt could be determined to an accuracy of approximately .3 milliseconds. With Δt ranging from 2.5 to 10 milliseconds depending on the type of wave and on the distance Δx between the observation points, the relative error for Δt was between 3 and 12 percent. Considering in addition that the absolute error of Δx was $\pm$ .1 cm and that Δx was usually from 5-10 cm, the largest possible relative error for a single speed measurement was between 4 and 13 percent. In each experiment generally 5 or more data points were analyzed at each frequency for each type of wave under the various conditions studied in this research and their results were averaged.

Guided by the observations in reference (18) regarding the attenuation of small amplitude sinusoidal pressure waves in the aorta, the ratio of the amplitudes of the various waves was evaluated as a function of the propagation distance Δx measured in wavelengths. The amplitude is defined as illustrated in Figure 16 and since A diminishes in an exponential fashion with distance, the ratio A/A_o is plotted on a logarithmic

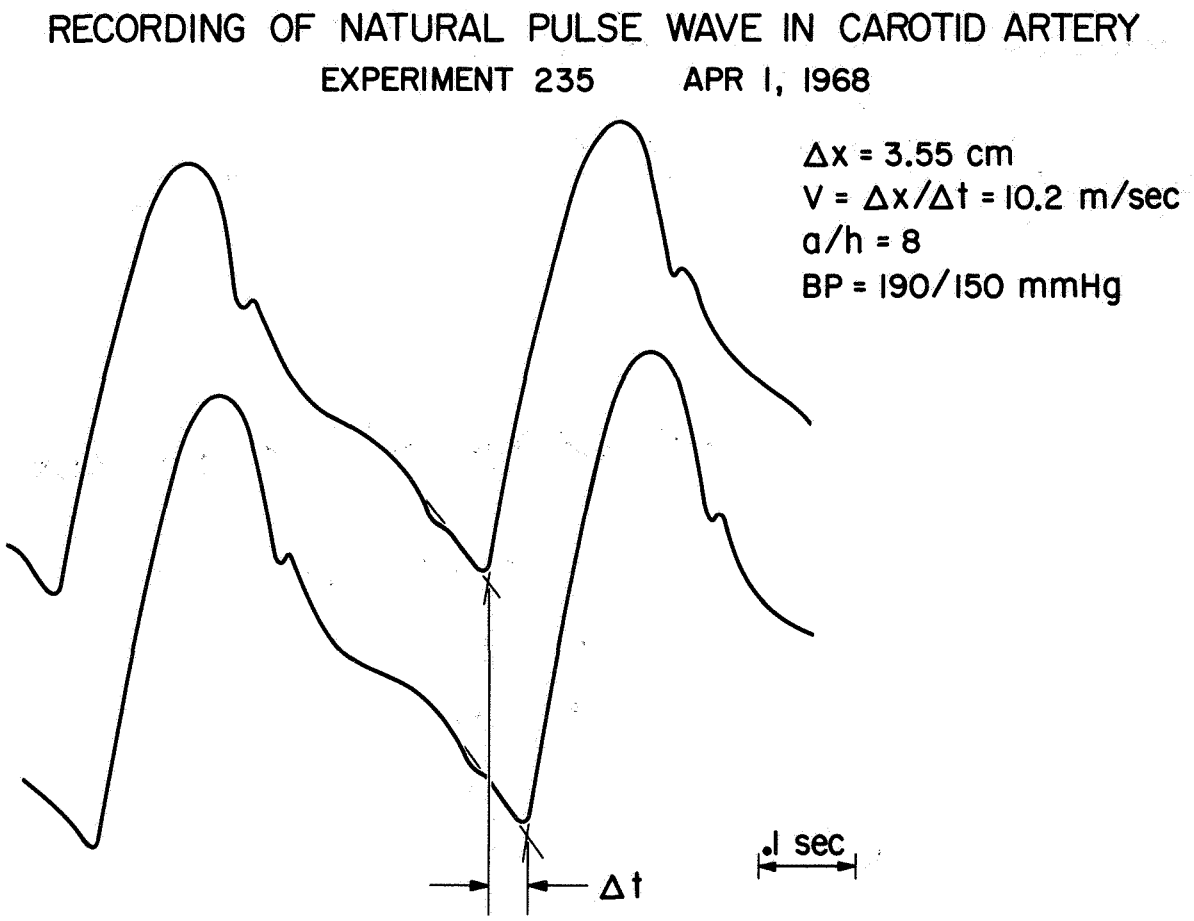

Figure 15. Representative tracing of natural pulse wave in right carotid. The pressure records were obtained with the aid of two pressure transducers of the kind shown in Figure 4. Δx denotes the distance between the needle-tips and Δt the corresponding transmission time. V = signal velocity, $\frac{a}{h}$ = radius to wall-thickness ratio and BP = blood pressure.

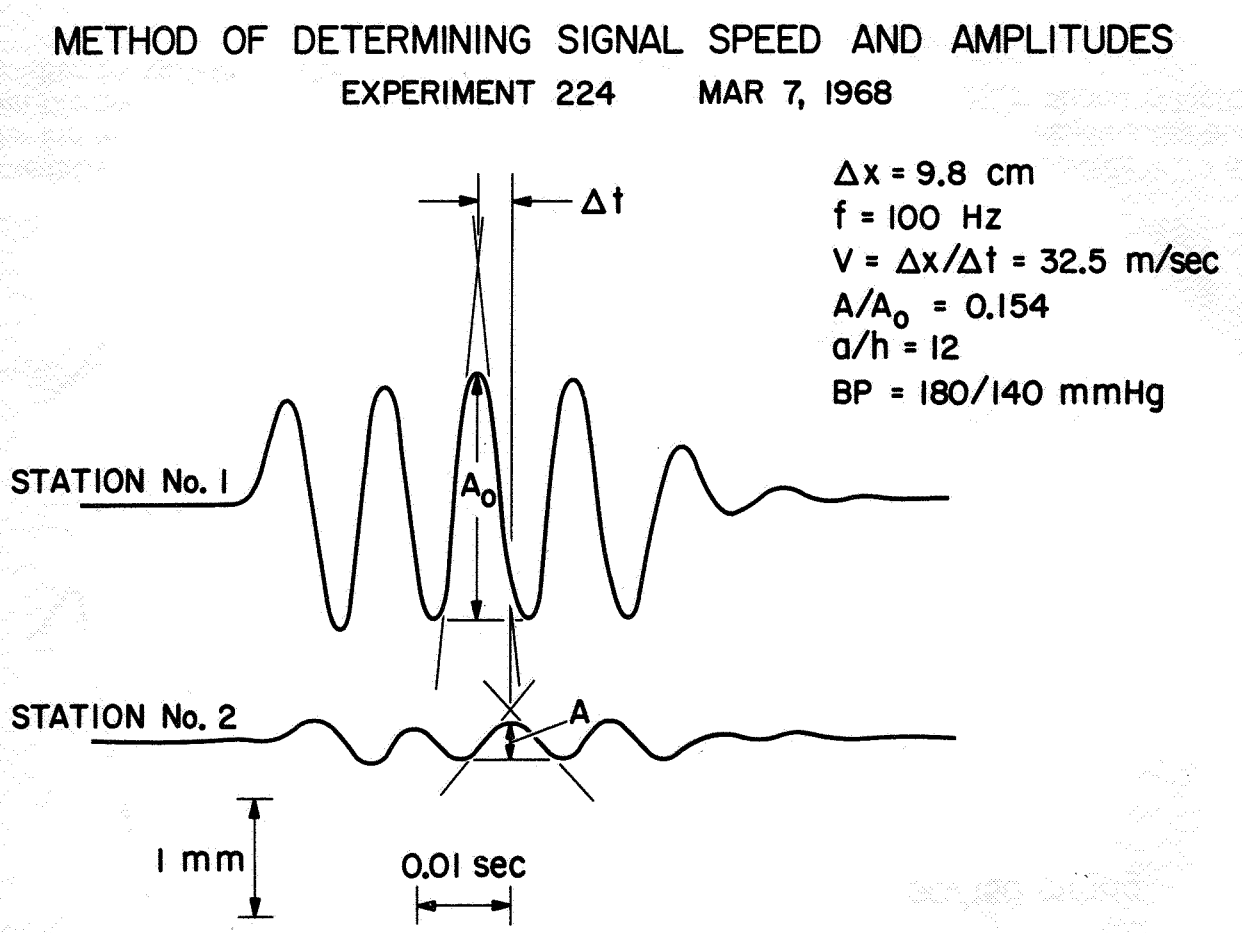

Figure 16. Tracing of artificially induced axial wall displacements in the form of finite trains of sine waves with a frequency of 100 Hz. As indicated, the signal speed is defined by the target separation Δx and the transmission time Δt of the intersection of the tangents in two successive inflection points. The peak-to-peak amplitudes of the sine waves are determined as shown. Note that the waves retain their sinusoidal character during propagation. The signals recorded for pressure and torsion waves were of the same form as shown in this figure.

scale versus $\Delta x/\lambda$ (λ = wavelength).

As a further check on the errors contained in the data, standard deviations were calculated for selected frequencies for each type of wave. Figures 19 and 20 have 95 percent confidence intervals drawn in for each type of wave at 50 Hz. These intervals indicate that 95 percent of all the data will fall within the bounds shown. Similar confidence intervals exist at higher and lower frequencies.

V. RESULTS AND DISCUSSION

The following six sections will present the results of the various studies conducted in the course of this research. Each section will contain a brief introduction and a description of the experimental technique used. The results for each wave will be given and discussed.

A. NATURAL PULSE WAVE SPEED AND NATURAL WALL DISPLACEMENTS

Data was acquired to determine the speed of the natural pressure pulse wave in the carotid artery under both unexposed and exposed conditions. In the unexposed case, a pair of capacitance pressure cells were inserted into the carotid artery by way of the cranial thyroid branch and positioned with the aid of an X-ray fluoroscope. Data was then taken at various Δx distances and in various regions of the neck.

The results indicate that the natural pressure pulse travels about 10-11 m/sec. No data was acquired on its damping characteristics although it can be safely said that the wave is only mildly damped.

To obtain the effect of the surrounding medium on the transmission of the pulse wave, the tissue was stripped away, completely exposing the vessel. Again data was acquired at various Δx's and in different regions of the neck. The results indicate a wave speed of about 10 m/sec. Thus, the effect of the surrounding medium on the speed of the natural pressure wave appears to be slight.

In addition, the speed of the pulse wave was determined using a pair of needle Bytrex pressure transducers described in Chapter III. These results may be summarized as follows: at normal blood pressure levels the speed of the natural pulse wave in the exposed carotid artery of 4 dogs was found to have an average value of 10.2 m/sec.

The wave speed was determined in all cases from pressure recordings such as that shown in Figure 15.

When the naturally occurring wall motion of the exposed artery is observed, it appears that the pressure pulse has associated with it an axial wave. Theoretically, then, it should be possible to determine the speed of the natural pressure wave from recordings of this axial wall motion. One might expect, however, that some of the observed wall displacement in the carotid artery results from the motion of the heart within the chest cavity during a normal cardiac cycle. It is therefore necessary to separate out the relative contributions of the pressure wave and the rigid body motion of the heart to the naturally occurring axial wall displacements.

This was accomplished by making an incision from the sternum to the region of the cranial thyroid branch and removing all tissue from around the carotid artery over the first 20 cm of its length. Targets were then attached at various locations up the artery from its origin. Data was taken on the natural axial wall motion, a typical sample of which is shown in Figure 17.

As can be seen from this figure, the amplitude of the naturally occurring axial wall displacement was on the order of .5 mm or less. In an effort to determine the relative contribution of the heart motion, a restraint was applied to the vessel which allowed for nearly unrestricted blood flow but no wall displacement. The plastic collar described in Chapter III was used for this purpose and was firmly anchored to the operating table. With the restraint applied 6.6 cm from the proximal station (No. 2 in Figure 17), the motion was reduced at both stations to approximately .13 mm.

It thus appears that the natural axial wall displacement observed in the exposed carotid artery is made up of two components--one due to the traveling pressure wave and the other due to the mechanical coupling of the motion of the heart to the upper part of the arterial tree. The component due to the pressure wave is approximately .13 mm in amplitude and is essentially undamped over a Δx of 10 cm while its shape is similar to that shown for Station 1 in Figure 17. Further, the motion of the heart in the chest cavity during the cardiac cycle results in motion in the wall of the carotid artery that is highly damped with distance from the heart and has a magnitude of approximately .4 mm at the root of the carotid artery. This component is so highly damped that it is essentially nonexistent half-way up the neck.

It was impossible to obtain the speed of the pressure wave from the above procedure of recording wall motion since there were no well defined points on both records (Station's 1 and 2) from which to determine time differences.

On subsequent experiments, an effort was made to measure any naturally occurring torsional wall motion. It was found that there was no detectable motion in the circumferential direction at any point on the exposed carotid artery between the brachiocephalic artery and the cranial

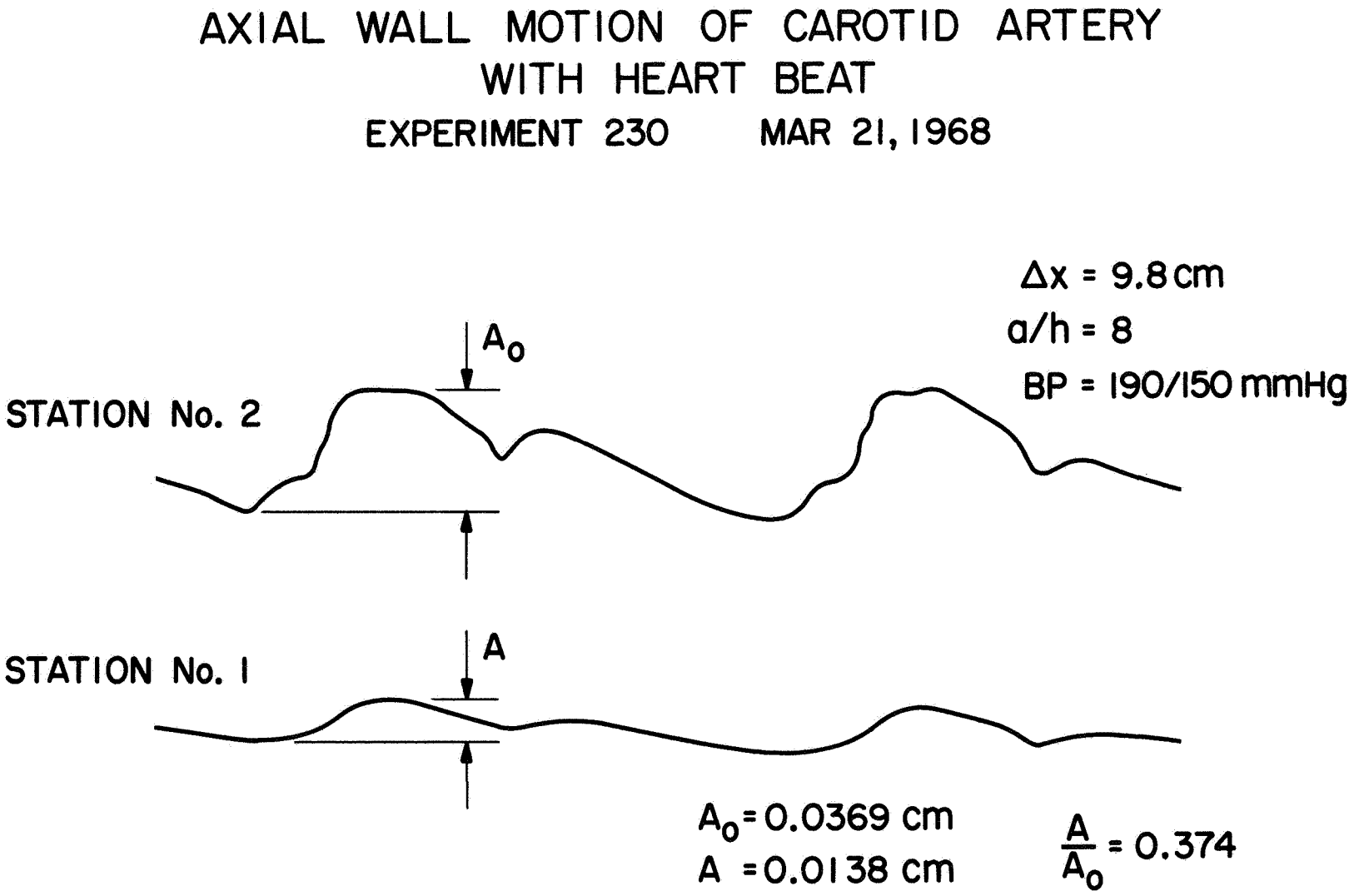

Figure 17. Tracing of axial wall motion of exposed carotid artery with heart beat. The motion was recorded with the aid of an electro-optical tracking system. Station 2 is nearer to the heart. Note strong attenuation.

thyroid branch.

Patel and Fry (23) have shown that the shearing strain induced by intraluminal pressure changes is small in the carotid artery and thus one would not expect to see torsional wall motion in response to naturally occurring pressure fluctuations. While their work was on an excised segment of artery, there appears to be no reason why their results can not be applied to the in-vivo case. Indeed, they reported some preliminary checks under in-vivo conditions which tend to confirm their results obtained on the excised segments.

B. DISPERSION AND ATTENUATION IN EXPOSED VESSELS

Introduction

The primary purpose of this research was to determine the phase velocity versus frequency (dispersion) relationships for the three types of waves and their damping characteristics. To this end, a series of six experiments (6 dogs) were conducted in which all three types of waves were generated in the exposed carotid artery and the speed and attenuation of the artifically induced waves were determined.

In each experiment care was taken to minimize the systematic error. Data was recorded in a short period of time (usually less than 30 minutes total elapsed time from the beginning to the end of data acquisition) and frequent checks were made to insure that the vessel wall had not changed materially during the course of the data run. This was done by monitoring waves of one type at intervals during data runs on another type. For instance, while taking data on torsion waves a series of axial waves of one frequency would be generated and their wall motions recorded. In the data analysis a check would then be made to see if there had been a significant change in the transmission characteristics of the other (i.e. axial in this case) type of wave while taking data on the particular wave under study at that time (i.e. torsion). In all cases, there was no change in the transmission characteristics that might reflect a change in the material properties of the vessel wall over the time period of interest.

In addition to these six experiments in which all three types of waves were generated, 25 other dogs were studied in which data on at least one type of wave was obtained. The results of all these experiments will be shown here.

While there were some individual variations, virtually all of the signals had the form shown in Figure 16 and were reduced as shown. In the case of pressure and axial waves, the amplitudes of the initial signals were kept small, i.e. within the linear range. Transmission characteristics of torsion waves, however, showed a marked dependence on A_o. A more detailed discussion of this will be given in Section D of this chapter.

The amplitude of the pressure waves were less than 10 mm Hg peak-to-peak while the torsion and axial waves were generally less than about

2 mm peak-to-peak. The frequency range covered was from 20 to 200 Hz with most of the data restricted to the range 20 to 100 Hz.

Histand (24) has reported noting a definite flow effect on the speed of the pressure wave in the aorta. Waves traveling with the flow had a consistently higher phase velocity than those being propagated against the flow. It was not possible to detect any such flow effect on the speed of pressure waves in the carotid artery. This observation may be the result of the particular experimental arrangement in my case. Virtually all of the results obtained using the capacitance pressure transducers were for waves traveling downstream while the needle Bytrices were used for studying waves traveling against the flow. The phase velocity of small amplitude pressure waves was in both cases the same, thus pointing to the absence of a flow effect on the speed of pressure waves in the carotid artery. However, the flow in the case of the catheter-tip manometers may have been substantially reduced due to the partial occlusion of the artery caused by the two 1 mm diameter catheters. In a vessel with an inside diameter of 3.5 mm, this would cause a 20 percent reduction in the area of the lumen. While it was initially felt that this would not adversely effect the results, it may indeed have prevented the detection of a flow effect similar to that found in the aorta.

It would then seem logical to use the needle Bytrices to monitor the speed of waves traveling downstream and verify the results. Unfortunately, the needle Bytrices failed early in the program and replacements were not available.

In addition, the apparent absence of a flow effect may be due to the fact that the peak flow velocity of the blood in the carotid artery is on the order of 1 m/sec (7) or less than 10 percent of the measured phase velocity. This amount of deviation can not be reliably distinguished by the methods of data analysis used in this research.

In the case of torsion and axial waves there was no detectable difference in the transmission characteristics between waves being propagated up or downstream. In addition, it was not possible to see any difference in the velocity and damping of these types of waves with blood pressure during the normal cardiac cycle. A more detailed discussion of pressure effects may be found in Section C.

The effects of various conditions such as the surrounding medium and changes in the transmural pressure are discussed in Sections C through F of this chapter. This section applies to results obtained on fully exposed arteries under normal blood pressure and natural initial stretch.

Dispersion

The results obtained from the above experiments are shown in Figures 18-20. Figure 18 shows the results obtained from one experiment while Figures 19 and 20 show the results averaged over the 6 and 25 experiments mentioned earlier.

Each data point shown in Figure 18 represents the average of at least 5 velocity determinations. Thus in Figure 19 where the results of 6 dogs are averaged each point represents the average of approximately 30 data points at any given frequency for each type of wave.

There may be some skepticism about the value of averaging the results from different dogs as has been done in Figures 19 and 20. It is obvious that physiological differences may be responsible for some, if not all, of any variations observed. As a check on the variability of the data between dogs, 95 percent confidence intervals have been calculated at selected frequencies--a sample of which is shown in Figures 19 and 20. Similar intervals exist at both higher and lower frequencies.

It should be pointed out here that it was not possible to correlate any measured differences in the speed of a particular type of wave between different dogs with such physical parameters as dog weight or vessel geometry. In addition, the age and medical history of each animal was unknown thus preventing any correlation on either of these bases.

The results shown in Figures 19 and 20 will be used in subsequent discussions in which the experimental results are compared with theoretical predictions. This is considered valid since even though there may have been variations between dogs, the results from all animals showed the same basic relationships between the transmission characteristics of the three types of waves and the dispersive character of each wave was essentially as shown in Figures 18-20.

All three graphs reveal first of all that the pressure wave is essentially nondispersive and has a speed approximately equal to 11 m/sec.

DISPERSION OF AXIAL, TORSION AND PRESSURE WAVES
IN EXPOSED CAROTID ARTERY

EXPERIMENT 326 OCTOBER 16, 1968

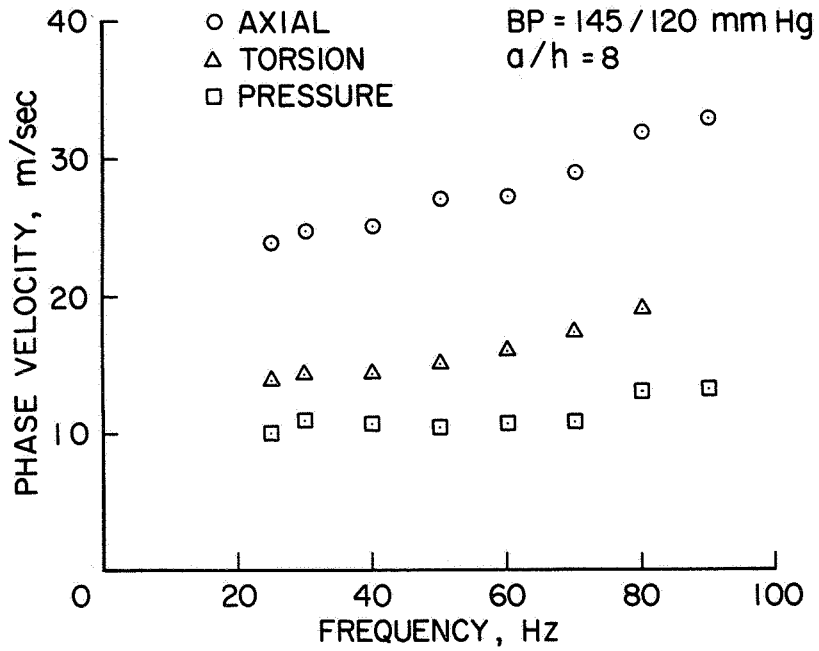

Figure 18. Dispersion of artificially induced axial, torsion and pressure waves in the exposed carotid artery of one dog. Each data point represents the average of at least 5 velocity determinations.

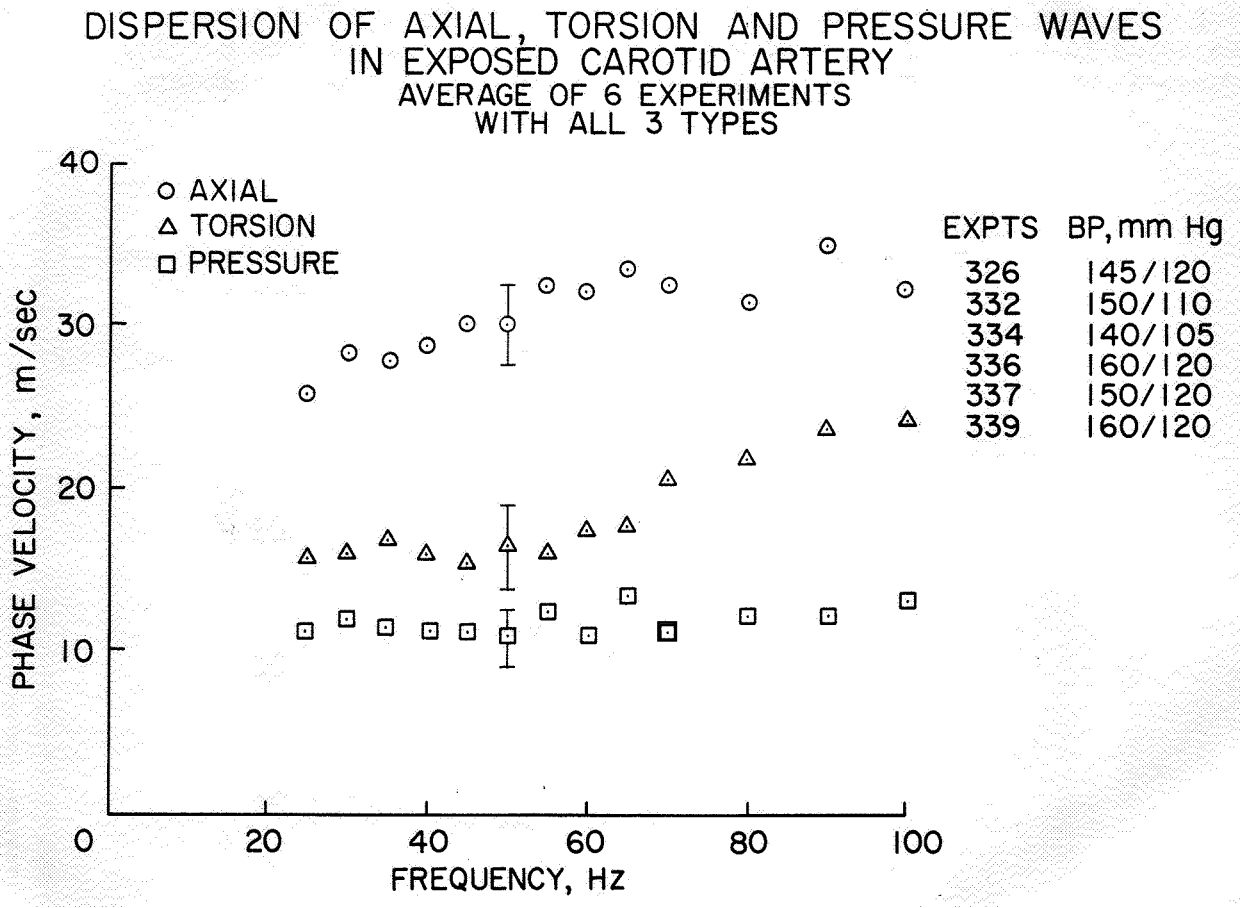

Figure 19. Average dispersion pattern of artificially induced axial, torsion and pressure waves in the exposed carotid artery of six dogs in which all three types of waves were studied. Each data point represents the average of approximately 30 velocity determinations. Also shown are the 95 percent confidence intervals for each type of wave at 50 Hz. Similar intervals exist at higher and lower frequencies.

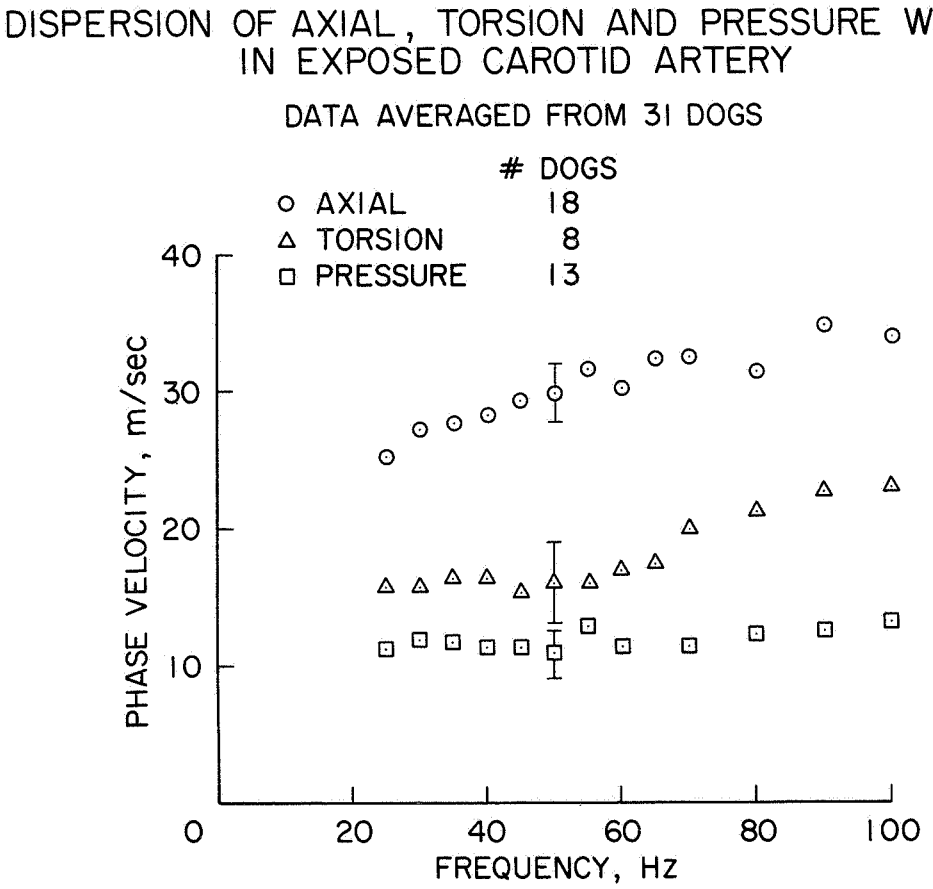

Figure 20. Average dispersion pattern of artificially induced axial, torsion and pressure waves in the exposed carotid artery of 31 dogs. Data on all three types of waves was not obtained from each dog but the information from Figures 18 and 19 have been included. Also shown are the 95 percent confidence intervals for each wave at 50 Hz. Similar intervals exist at higher and lower frequencies.

While individual dogs showed slight variations from this average, the results were in all cases non-dispersive. In addition, pressure waves were studied at frequencies up to 200 Hz. The results of these experiments also confirm the nondispersive nature of artificially induced pressure waves of small amplitude in the carotid artery in the frequency range 20 to 200 Hz. In reference (18) it has been shown that the aorta also behaves in this manner (nondispersive).

It is of interest to note that the results given in Section A show that the average speed of the natural pressure wave is 10-11 m/sec--also very close to that determined here for artificial waves.

The dispersive nature of the carotid artery with respect to torsion waves is somewhat more complicated. At frequencies between 20 and 50 Hz the curve is essentially flat. Above 50 Hz the velocity increases with increasing frequency. The speed of the torsion waves varies from about 16 m/sec at low frequencies (below 50 Hz) to about 24 m/sec at 100 Hz. While this increase may at first seem large, it still falls within our definition of a mildly dispersive behavior (see Chapter II).

There were problems in acquiring torsion wave data which merit some discussion. The greatest difficulty encountered in the generation of torsion waves was in eliminating the occurrence of a transverse wave (i.e. a vibration perpendicular to the vessel's longitudinal axis). It appears that this wave may be easily generated if the torsion wave exciter is slightly misaligned with the axis of the vessel. The occurrence of these waves was generally easy to recognize due to the fact that the amplitude of the signal at the second station was almost always larger than that at the first. It was found that proper alignment of the shaker would eliminate these spurious signals.

The attenuation characteristics of the torsion waves also made their study difficult. At any given frequency, their damping was much higher than that of either pressure or axial waves. In addition, there was a rather sensitive amplitude dependence on the damping which will be described in Section D of this chapter. It was necessary to place the first target about 2 cm from the shaker and restrict Δx to values less than 5 cm. It thus becomes almost impossible to monitor both torsion and axial waves simultaneously with any degree of reliability in the

time delay measurements of the axial wave.

As can be seen from Figure 20, the dispersive nature of axial waves is more uniform than that of the torsion waves. The phase velocity increases with increasing frequency and ranges from 25 m/sec at 25 Hz to about 35 m/sec at 100 Hz. In some experiments data was taken up to frequencies of 150 Hz and the speed was found to average 40 m/sec at that frequency. Thus the behavior of the axial wave is also mildly dispersive.

From the recordings of the artificially induced waves of all three types it can be seen that the finite trains of sine waves retain their sinusoidal character during propagation for all the frequencies covered in this investigation. This may be interpreted as a further indication that the carotid artery is not strongly dispersive with respect to axisymmetric waves of all three types in the frequency range covered. Further substantiation of this conclusion is the independence of the transmission time Δt with respect to the selection of the characteristic point on the train. Since there is a weak frequency dependence of the signal speed for all three types of waves, the corresponding velocities may be interpreted as a good approximation to the corresponding phase velocity. As expected on the basis of theoretical studies (13,25,26), the phase velocity of the axial and torsion waves increases with increasing frequency in the case of viscoelastic models for the vessel wall such as the Voigt model used by Maxwell and Anliker (13). A purely elastic analysis predicts that there will be no dispersion whatsoever for axisymmetric torsion and axial waves when the blood is considered inviscid. (See Chapter I for a discussion of the effect of viscosity on pressure and axial waves.)

When the dispersion results shown in the figures are compared with the theoretical predictions mentioned in the preceeding paragraph it is readily apparent that, over the frequency range covered in these experiments, the axial and torsion waves travel at a slower speed relative to the speed of the pressure wave than they should. Anliker and Maxwell's (12) elastic analysis predicts that the axial wave should travel at approximately 5 times the speed of the pressure wave while the torsion wave should travel almost three times as fast. In addition, as mentioned above, the isotropic model for the vessel wall does not predict any dispersion.

When Maxwell and Anliker's viscoelastic (Voigt) model is considered,

we again see a similar discrepency between the predicted wave speeds and those measured in this study. The theoretical results indicate that with a pressure wave speed of 11 m/sec at 50 Hz the axial wave should travel at 60 m/sec and the torsion wave about 30 m/sec. As can be seen from Figure 19 the axial wave travels about 30 m/sec while the torsion wave speed is 17 m/sec at this frequency.

This large discrepency between the predicted and measured wave speeds indicates an anisotropic behavior of the vessel wall. Specifically, the vessel appears to be approximately twice as elastic in the axial as in the circumferential direction.

There has been a considerable amount of work performed on excised arterial segments (for instance Patel et al (27)) and some work on arterial segments in-situ (Patel and Fry (28)). Some of this work, particularly that of Fenn (29), has found that the vessel appears to be more elastic (have a lower Young's modulus) in the axial than in the circumferential direction. To the best of my knowledge, the conclusions reached in the preceeding paragraph are the first in-vivo experimental evidence to support the idea that the material properties of the vessel wall are not the same in all directions--that is to say, the vessel appears to be nonisotropic.

Attenuation

The damping characteristics of the three types of waves are shown in Figures 21-23. Figure 21 shows the results from one animal in which all three types of waves were generated while Figures 22 and 23 show the results averaged over the 6 and 31 experiments respectively.

When the amplitude ratio A/A_o is plotted as a function of the distance traveled in wavelengths, it can be seen that the functional relationship is approximately $A/A_o = \exp(-k\ \Delta x/\lambda)$ where k is the logarithmic decrement and is essentially independent of frequency for all three types of waves and λ is the wavelength of the wave.

It should be pointed out here that the results shown for the axial and pressure waves were virtually independent of the initial amplitude of the signals within the range covered. However, the damping characteristics of the torsion wave are much more sensitive to the magnitude of A_o. A complete discussion of amplitude dependence will be given in Section D of

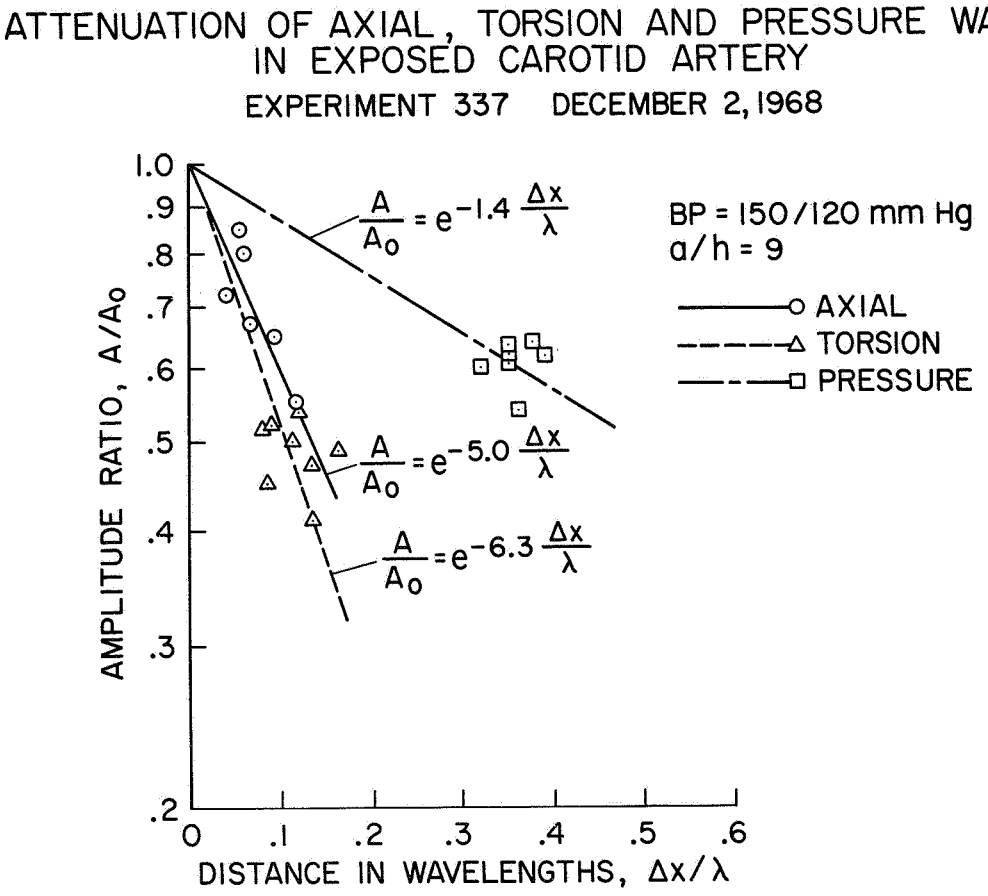

Figure 21. Representative attenuation pattern observed for the three types of waves in the exposed carotid artery of one dog. Each point corresponds to the average of at least 5 individual measurements. The data was obtained by holding Δx constant and varying the frequency and thus the distance traveled in wavelengths. The value of A_o for the torsion waves was maintained at approximately .8 mm.

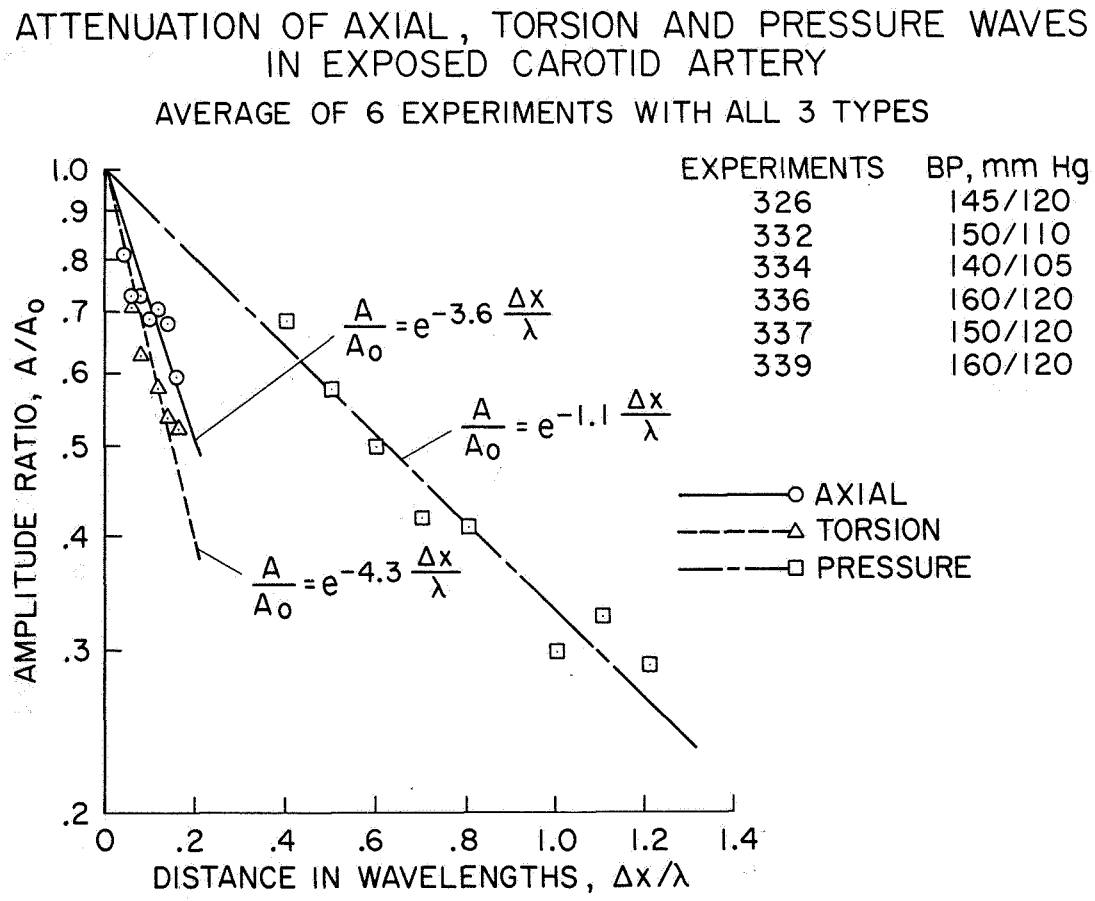

Figure 22. Average attenuation ratio from six dogs in which all three types of waves were studied plotted as a function of the distance traveled in wavelengths.

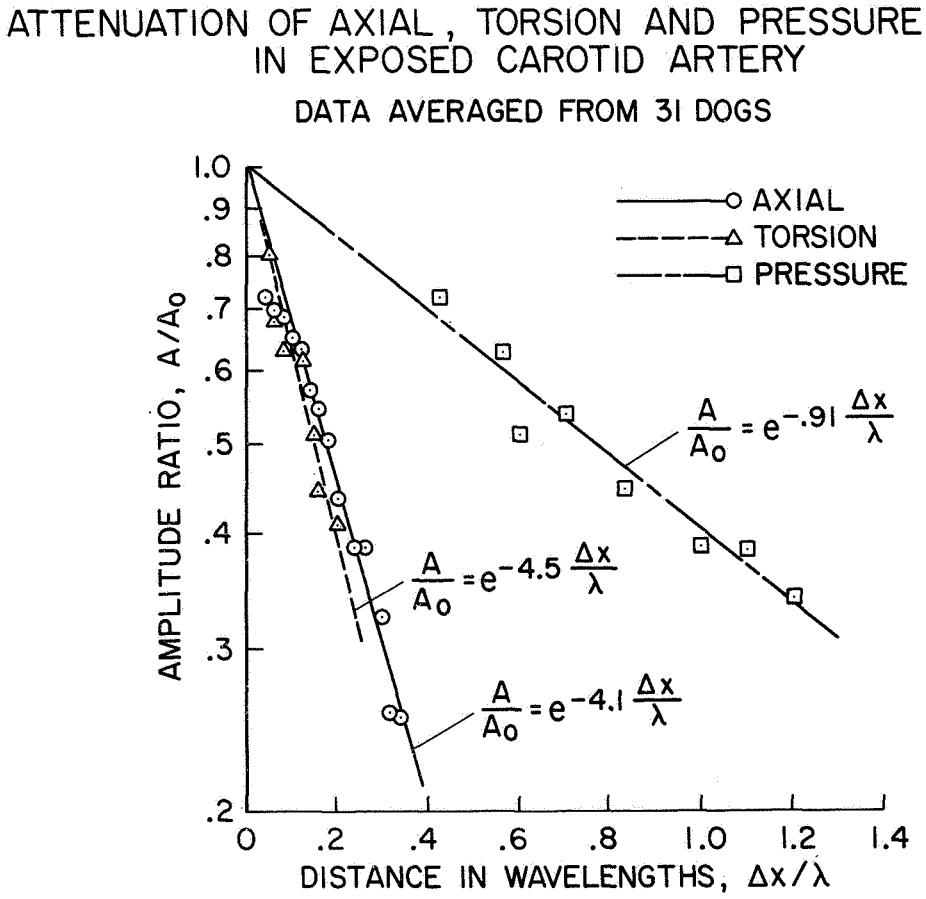

Figure 23. Average attenuation pattern of artificially induced axial, torsion and pressure waves in the exposed carotid artery of the 31 dogs mentioned in Figure 20.

this chapter. The initial amplitude of the torsion waves used to obtain the data in Figures 21-23 was approximately equal to .8 mm and was held constant for all frequencies. The results of the torsion wave damping should be used with care since there appears to be a rather strong amplitude dependence for this particular wave.

While it is convenient to plot the attenuation as shown in Figures 21-23, this manner of presentation tends to obscure the fact that even though the axial and torsion waves appear to be equally damped per wavelength, the torsion wave is much more highly damped than the axial wave per Δx. This of course results from the vastly different speeds and thus different wavelengths for the two waves. The axial wave is actually transmitted over a much longer distance than is the torsion wave for any given A_o.

There are basically three possible contributions to the damping of any type of wave in any vessel. First is the radiation of energy into the surrounding medium. The second is the viscous effects of the blood in the blood vessel. And third is the viscoelastic damping of the vessel wall itself. Since our vessels in this case were completely exposed, the possibility of radiation can be neglected. As far as blood viscosity effects are concerned, Jones et al (14) have shown that this too can account for only a small fraction of the damping present. It thus appears that the viscous damping mechanism of the vessel wall is largely responsible for the damping of waves of all three types.

The viscoelastic wall models allow for an E in the form $\hat{E} = \hat{E}_r(\omega) + \hat{E}_i(\omega)$ where $\hat{E}_r(\omega)$ is a function of frequency and is primarily the determining factor of the dispersive character of the vessel while $\hat{E}_i(\omega)$ is also frequency dependent and determines the damping. In reference (13) they selected the Voigt model in shear, for which $\hat{E} = 3(E_o - i\omega\eta)$, where E_o is the elastic parameter and η is the viscous parameter in the model.

Using the approximations given in reference (13) for the case of $\hat{\omega}\hat{\eta}$ much less than one and h/a also much less than one, it is possible to estimate the value of the parameter $\hat{\eta}$, the nondimensional coefficient of wall viscosity. If this is done, $\hat{\eta}$ for the axial and torsion waves is found to be approximately 5.0 using k = 4 while for the pressure waves (k = 1) we find $\hat{\eta} = 2.0$. Both of these values exceed the maximum value considered by Maxwell and Anliker ($\hat{\eta} = 1.0$) and indeed reflects quite a high wall viscosity.

Maxwell and Anliker's results also indicate that the damping of all three types of waves will be frequency dependent at low frequencies. The results shown here seem to indicate rather strongly that this is not the case.

C. TRANSMURAL PRESSURE EFFECTS ON THE TRANSMISSION CHARACTERISTICS

Introduction

Theoretical studies taken from reference (13) indicate that for the viscoelastic model of the artery wall used therein, increasing the transmural pressure by a factor of two should increase the speed of both the axial and torsion waves but will not effect too significantly the speed of pressure waves at low frequencies. In addition, the damping per wavelength is not effected to any large extent by changes in the transmural pressure for all three types of waves.

Experimental results on the speed of the pressure wave in the thoracic aorta by Anliker et al (18) indicate that between systole and distole there can be a 50 percent increase in the speed of the induced pressure waves. That is, with a blood pressure of 100/65 mm Hg, the speed at diastole was approximately 4 m/sec while at systole it was 6 m/sec.

In order to check for the existence of a similar effect in the carotid artery a series of experiments were conducted to determine how arterial pressure changes effect the dispersion and attenuation of the three types of waves.

Experimental Procedure

The experimental procedure involved three techniques to change the transmural pressure. In the first, a balloon firmly attached to the end of a radio-opaque catheter was inserted into the femoral artery and advanced into the thoracic aorta with the aid of the X-ray fluoroscope. The end of the catheter was positioned approximately adjacent to the heart. Upon inflation, the balloon would restrict flow down the aorta and cause a subsequent pressure rise in the upper part of the arterial tree. Pressure rises of 50 to 70 mm Hg above the normal mean blood pressure were easily obtained by this technique.

When the balloon was deflated, the blood pressure in the carotid artery would fall to a level well below the normal mean blood pressure that existed prior to inflation. This was due to a decreased blood volume in the distal arteries (that is, vessels downstream from the balloon) as a

consequence of run-off into the capillaries and veins. The level of the blood pressure in the carotid artery after deflation of the balloon was commonly 30-50 mm Hg below the normal mean blood pressure. Thus changes in the transmural pressure on the order of 100 mm Hg were easily obtained by the use of this technique. Data on the transmission characteristics of each wave were taken continuously over the 10-20 second interval during which the pressure rose and then fell.

Occlusion of the carotid artery was the second method employed. A piece of umbilical tape would be looped around the vessel at a point above the cranial thyroid branch. When the ends of the piece of tape were pulled the loop would close and occlude the vessel. This occlusion, together with the carotid sinus reflex, would cause the pressure to rise about 50-80 mm Hg above the natural, unoccluded blood pressure. When the loop was released the pressure would quickly return to normal without the undershoot mentioned above in connection with the balloon catheter.

This method (occlusion) when used in conjunction with the balloon allowed for a check on whether any increases in speed (particularly of pressure waves) was the result of pressure or flow or both. When the carotid artery was occluded the flow would of course cease but the pressure would rise. When the balloon was inflated, the pressure and flow could both be expected to rise.

The third method that was occasionally used was vagal nerve stimulation by means of a Grass Instrument Co. Stimulator Model S4C. The right vagus nerve was exposed and a biphasic electrical potential of 10 volts, 20 Hz frequency and 5-10 milliseconds in duration was applied. The object of this was to induce electrical impulses in the vagus nerve that would temporarily stop the heart. With the heart stopped, the blood pressure in the entire arterial tree would decrease.

This technique had certain limitations and drawbacks. The foremost limitation was that it was possible only to decrease the blood pressure so that no information could be obtained on high pressure effects. In addition, difficulty was also encountered in obtaining the proper combination of voltage, frequency and duration that would stop the heart. These parameters seemed to vary somewhat between dogs. In some dogs it was necessary to sever the nerve and stimulate its distal end to secure the desired car-

diac arrest. Indeed, in some cases the heart could not be stopped .

In addition, it was found that stimulation of the vagus nerve would cause severe muscular contraction in the necks of some animals. When studying pressure waves this was not a serious handicap. However, when trying to use the optical tracking units the motion induced by the muscle contractions would cause the targets to move out of the field of view.

With these considerations in mind, the bulk of the data reported in this section was taken using the balloon catheter and occlusion techniques.

Results

Natural Pressure Wave

In two of 13 experiments data was obtained using the capacitance pressure cells placed at various Δx's to determine the effect of varying the mean pressure on the speed of the natural pressure wave. The method of determining this speed has been discussed in Chapter IV.

The results of these experiments show that increasing the mean pressure by roughly 70 mm Hg resulted in a 50 percent increase in the speed of the natural pressure wave. In Experiment 352, for example, at Δx's of 4, 6 and 8 cm, the natural pressure pulse traveled at an average of 10.9 m/sec under normal blood pressure conditions (150/120 mm Hg). By the use of the balloon catheter technique the diastolic pressure was raised to approximately 170 mm Hg and had a subsequent fall to about 100 mm Hg. At 100 mm Hg the speed of the pulse wave was approximately 8.4 m/sec while at 170 mm Hg the speed had increased to 12 m/sec.

Figure 24 shows the results of these experiments. It can be seen that the results from both experiments are very similar and that increasing the diastolic pressure does indeed cause an increase in the speed of the natural pressure wave. In addition, data was taken both with and without the surrounding tissue in place and the results shown in the figure did not change.

Artificial Pressure Waves

When pressure waves in the form of finite trains of sine waves of

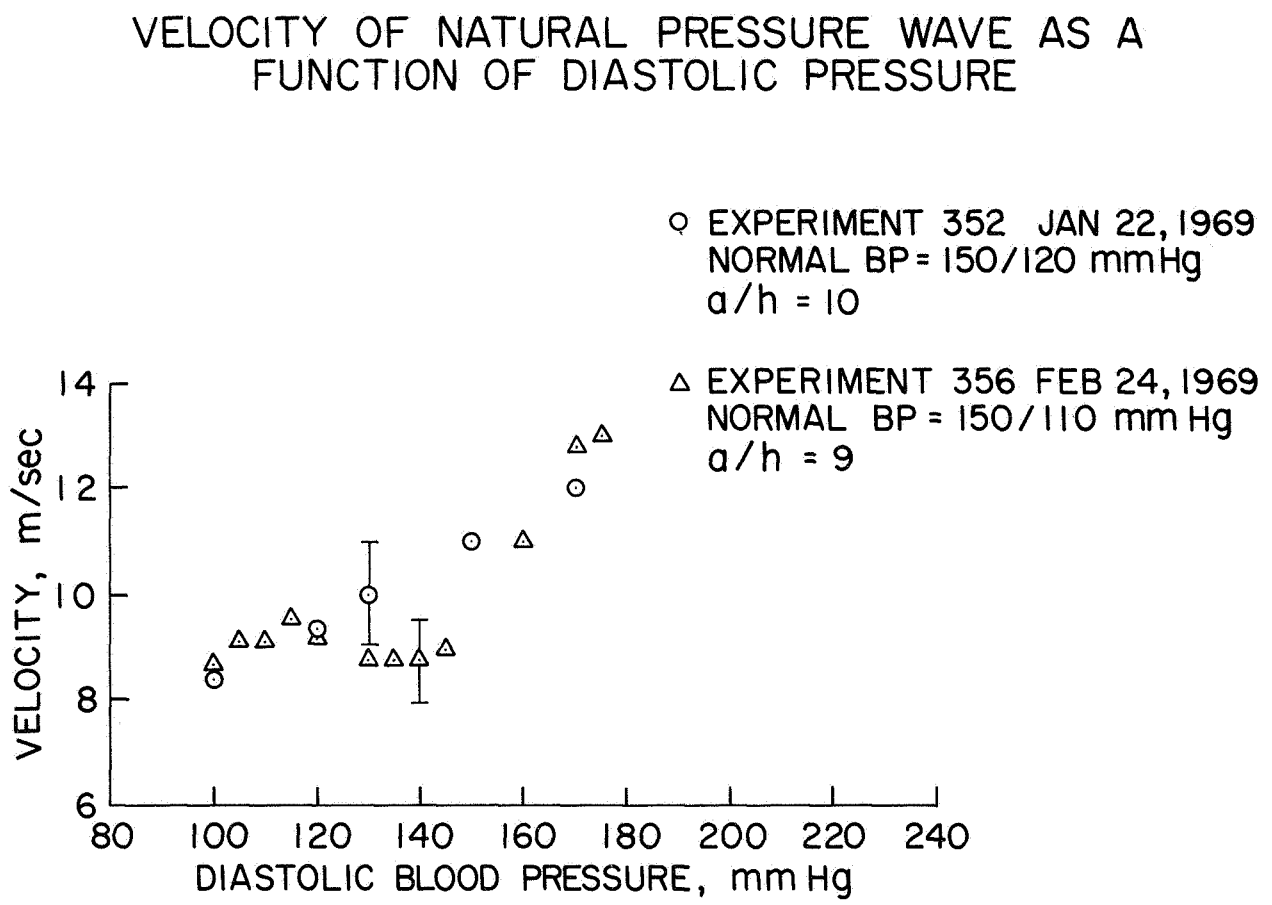

Figure 24. Speed of the natural pulse wave as a function of the diastolic pressure level in the carotid artery. The results of two experiments are shown. Each point represents the average of at least 4 velocity determinations. Typical 95 percent confidence intervals are shown.

small amplitude were induced in the carotid artery and the transmural pressure was varied, results similar to that obtained on the natural pressure wave were found. The speed of these waves increased with increasing pressure at a constant frequency and amplitude. (See Figure 25.)

One of the experiments shown in the figure was performed using the balloon catheter while the other made use of the carotid occlusion technique. Thus there was a significant difference between the conditions which existed in the two experiments. In the former both the pressure and flow in the artery were increased while in the latter only the pressure was raised. From Figure 25 it appears that the results of both experiments are quite similar. In both animals the speed of the naturally occurring pressure wave was almost identical (10 m/sec).

These results indicate that the arterial pressure is the dominant factor in determining the phase velocity of small amplitude pressure waves. Changes in the arterial pressure appear then to directly effect the material properties of the vessel wall.

When one considers the damping of artifically induced pressure waves it at first appears that the damping decreases markedly with increasing pressure (i.e. from an A/A_o = .57 at 120 mm Hg to A/A_o = .72 at 200 mm Hg). However, the logarithmic decrement, k, computed in the two cases is .63 at 120 mm Hg and .70 at 200 mm Hg. These values are so close because the speed of the wave increases with increasing pressure and thus the wavelength also increases (at a constant frequency). The faster wave would then not have traveled through as many wavelengths as the slower wave over the same Δx.

It thus appears that the damping of the artificial pressure wave is not markedly changed when the transmural pressure is varied within the ranges covered in these experiments.

Torsion and Axial Waves

Torsion and axial waves can be considered at the same time since their behavior in response to changes in the transmural pressure were identical over the pressure ranges covered in these experiments. In 4 experiments the pressure was varied as discussed above and data were taken on the speed and damping of torsion and axial waves as a function of the

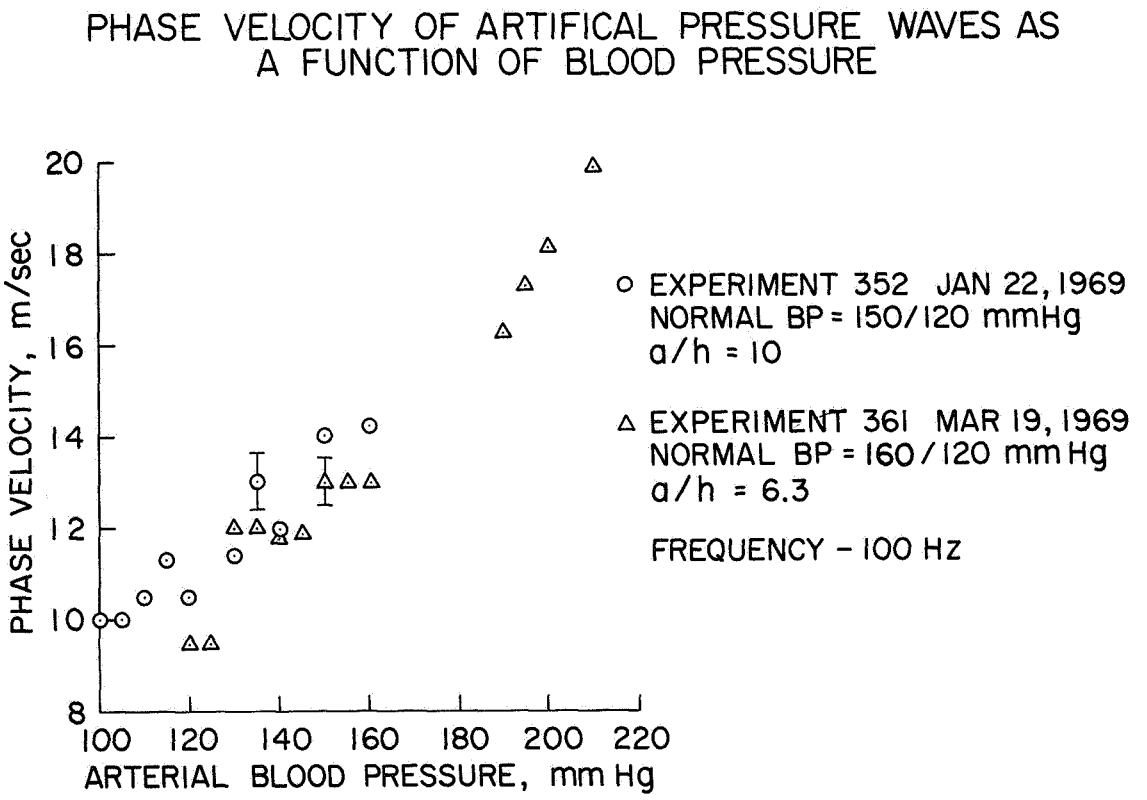

Figure 25. Phase velocity of artificial pressure waves in the exposed carotid artery as a function of the instantaneous blood pressure. The results of two experiments are shown. In one (352) the blood pressure was varied by the balloon catheter technique while in the other (361) the occlusion method was used. Both of these methods are described in the text. Each point represents the average of at least 3 velocity measurements. 95 percent confidence intervals are shown.

transmural pressure. The Δx's varied from 3 to 5 cm for torsion waves and from 5 to 10 cm for axial waves. The frequencies used were 30-50 Hz for torsion and 100 Hz generally for axial waves. Again the induced changes in transmural pressure were on the order of 100 mm Hg.

The results of these experiments may be summarized as follows: for the range of induced transmural pressure changes studied, the transmission characteristics of axial and torsion waves at a given frequency did not vary enough to be detected by the method of data acquisition and analysis used in these experiments. It follows also that there were no observable changes in the dispersion and attenuation of torsion and axial waves during different parts of the cardiac cycle.

Discussion

The above results conflict with the theoretical predictions mentioned at the beginning of this section. The transmission characteristics of pressure waves (both large amplitude, natural pulse waves and small amplitude, artificially induced waves) are quite sensitive to arterial pressure changes while the axial and torsion waves seem to be uneffected by changes in the blood pressure. It thus appears that increases in the transmural pressure cause material property changes in such a way as to effect many the transmission of pressure waves. In addition, it appears that changes in the flow that one would expect with increasing blood pressure have little effect on the speed of all three types of waves.

D. EFFECT OF VARYING AMPLITUDE

Introduction

One manifestation of a nonlinear behavior of any system is the dependence of the magnitude of the output of the system to the input. If the system is linear, then doubling the input will double the output and the ratio A_o/A_i would remain constant. A nonlinear system would then exhibit a variation in the ratio A_o/A_i with warying A_i. Another indication for nonlinearity of a material is a variation in the speed of a wave transmitted through it with changes in the wave amplitude.

Indeed, there appears to be increasing evidence that the arterial walls exhibit a nonlinear behavior (17,30), at least in response to the natural pulse. Bergel (31) has shown that the Young's modulus of arterial segments under static load conditions appears to vary with changes in the internal pressure.

Yet the vast majority of theories on the wave transmission characteristics of blood vessels assume that the vessel wall behaves in a linear fashion. The crucial question in applying these theories then becomes to what extent are the vessel walls nonlinear?

With these considerations in mind the initial amplitude of the various types of waves studied in this research were varied from near zero to the levels quoted in Chapter III. To repeat them here for convenience: pressure waves were generally limited to peak-to-peak amplitudes less than 10 mm Hg, torsion waves less than 1.5 mm wall displacement and axial waves less than 2.0 mm peak-to-peak. The amplitudes of all three types of waves were increased even beyond these levels in an effort to detect any amplitude dependence.

Results

Pressure Waves

In 4 experiments the amplitude of the pressure signals was increased at least five fold (i.e. from 2 mm Hg to 10 mm Hg peak-to-peak) and the dispersion and attenuation were determined. The various input amplitudes were easily obtained by simply varying the stroke of the piston attached

to the electromagnetic shaker. In each case, constant Δx and frequency were maintained.

The results of these studies indicate that there was virtually no change in the phase velocity with the imposed initial amplitudes. For instance, in one experiment the speed varied less than 5 percent from the lowest amplitude used to the highest.

The attenuation also exhibited a similar independence of initial amplitude. In this case the changes in A/A_o were typically less than three percent.

In some experiments the amplitudes were increased even more than described above in an effort to see some nonlinear effect. The results indicate that for artificial pressure waves with amplitudes up to 1/2 the pulse pressure (in some cases 20 mm Hg) there was virtually no effect on either the phase velocity or damping.

Torsion Waves

Figure 26 shows the results of three experiments in which the torsion wall motion was increased from about .4 mm up to a maximum of 1.6 mm peak-to-peak. In addition, a scale showing the approximate rotation in degrees corresponding to the various wall displacements is given. An outside diameter of 4 mm was used to make this conversion from mm to degrees. In all cases the frequency was held constant at 40 Hz.

It can be seen from the figure that increasing the initial amplitude of the torsion wave caused a significant increase in the ratio A/A_o. In one case (Experiment 349) the ratio increased from .42 at an A_o of .5 mm to .72 at 1.3 mm. It thus appears that the attenuation of the torsion waves is rather strongly dependent on the initial amplitude.

The speed of the torsion wave was not significantly effected however. For instance, in Experiment 361 the speed at A_o = .4 mm was 16.6 m/sec while at A_o = 1.0 mm the velocity was 17.3 m/sec and at A_o = 1.6 mm the phase velocity was 16.6 m/sec. Due to the consistency in speed the wavelength of the various waves would remain essentially constant. Thus, the ratio $\Delta x/\lambda$ would not change with increasing A/A_o. Therefore the decreased damping must be reflected in a decrease of the logarithmic decrement, k. The data from Experiment 354 yields the following k values: at

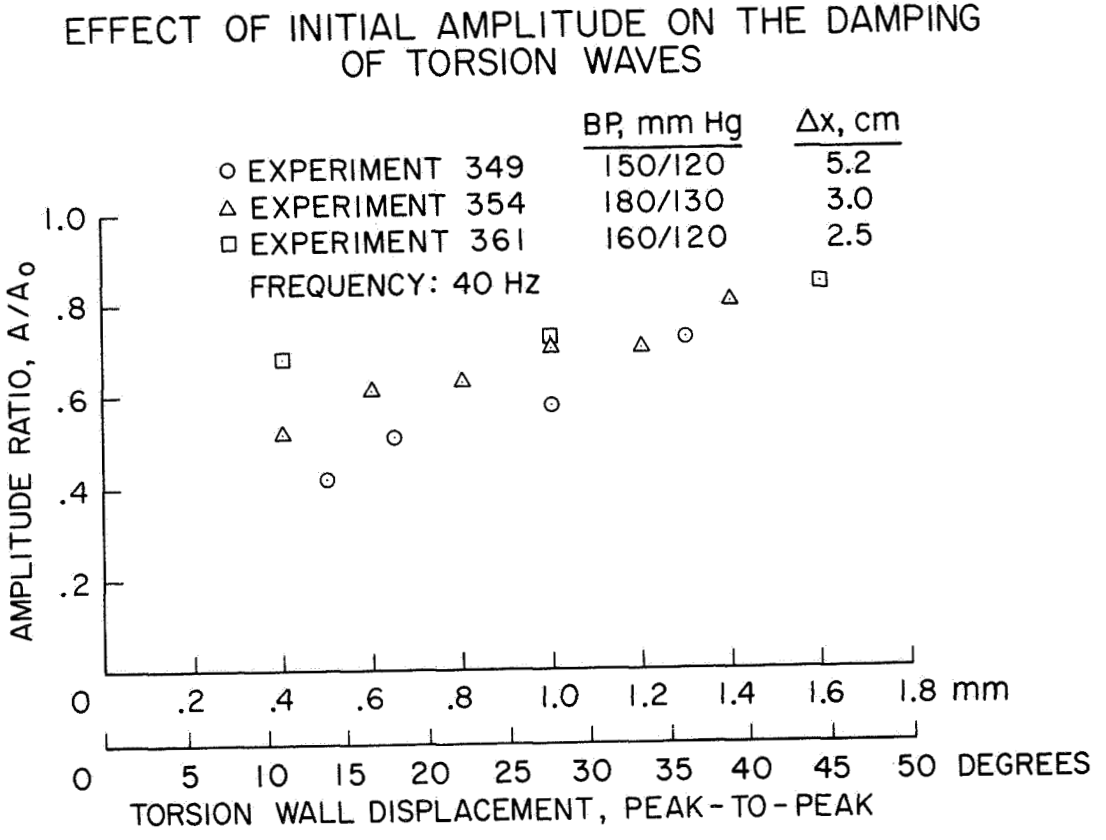

Figure 26. Variation of the damping of torsion waves as a function of initial amplitude. The wall displacements have been plotted in both millimeters and degrees, peak-to-peak. The conversion between the two units was made on the basis of a vessel whose outside diameter is 4 mm. The results from three experiments are shown.

A_o = .4 mm, k = 8; for A_o = 1.0 mm, k = 4.7; while for A_o = 1.4 mm, k = 3. It thus becomes obvious that the initial amplitude of the torsion waves is an important parameter in determining its attenuation.

Axial Waves

The amplitude dependence of the axial waves was analogous to that of the pressure waves. Changes in amplitude from fractions of a mm (.2) to 2.5 mm or slightly higher in some cases resulted in no discernable change in the transmission characteristics. In 5 dogs data was taken at various frequencies and over various Δx's within the ranges given in Chapter III.

Discussion

The following summary statements seem in order on the basis of the above results. The phase velocity of all three types of waves appear to be independent of the initial amplitude over the range of amplitudes covered by these experiments. The attenuation of pressure and axial waves does not seem to be dependent on the value of A_o. The damping of torsion waves can, however, vary dramatically with changes in the value of the initial amplitude. The vessel thus appears to be nonlinear with respect to torsion waves while reasonable linear for axial and pressure waves. These statements of course only apply in the range of frequencies and amplitudes given for each type of wave.

E. THE EFFECT OF VARYING INITIAL STRETCH

Introduction

A parameter which may effect the transmission characteristics is the initial stretch of the vessel. Table I shows that the carotid artery, in-vivo, is stretched between 1.2 and 1.6 times its excised length. The average value of $\Delta l/l_o$ is about 0.4. Thus the vessel in its natural state is highly stressed in the longitudinal direction.

It would seem logical that if this stress were varied then the vessel's initial stiffness would change and that such a change might be reflected in a change in the transmission characteristics of the various types of waves. Indeed, Maxwell and Anliker (13) have varied this parameter (q_1 in their analysis) and have shown that in the elastic case pressure waves exhibit relatively mild changes in phase velocity for changes in q_1 by a factor of 2 (.1 to .2). Torsion waves exhibit a stronger dependence on the q_1 parameter but again changes from .2 to .4 result in speed changes of less than 10 percent. Axial waves fall somewhere in between pressure and torsion waves as far as the magnitude of changes in the phase velocity with respect to changes in q_1.

When we consider the viscoelastic case, even though the definition of the stretch parameter changes slightly from that found in the elastic model, the behavior of the three types of waves is essentially the same as in the elastic case.

Maxwell and Anliker's results for the damping of the three types of waves in the viscoelastic model reveal that the axial wave damping is essentially uneffected by changes in q_1 from 0 to .4, Similar changes in the stretch parameter effect the transmission of torsion waves much more strongly, particularly at high frequencies. Likewise a change from 0 to .4 in q_1 will cause very large changes in the transmission of pressure waves, again at higher frequencies. In all cases when the frequency is near zero, the effect of changes in the q_1 parameter are negligible.

An analysis of the stress-strain behavior of the carotid artery was conducted in an effort to determine the approximate values of the stretch parameter. This was accomplished by excising a segment of the artery which had been drained of blood and placing it in a vertical test

jig. The ends of the artery were securely fastened with surgical thread for easy attachment to the test stand and to the loading pan into which weights were placed. Various loads were then applied to the vessel and the corresponding change in length was recorded along with the applied load. The results are shown in Figure 27, plotted as load applied in dynes versus extension from the excised length in cm. Note that a force of approximately 34,000 dynes was necessary to return the vessel to its in-vivo length.

The data shown in Figure 27 along with the physical dimensions of the specimen were used to calculate the stress-strain curve shown in Figure 28. In this analysis a Poisson's ratio of .5 was used and changes in the cross-sectional area of the vessel wall due to increases in the length were accounted for in determining the stress. This curve is based on the classical definition of strain $\epsilon = \Delta x/x_o$ where x_o is the original, excised length and Δx represents the total change in length under the applied load.

From the classical definition of Young's modulus, E = stress/strain, we find that $E = 3 \times 10^6$ dynes/cm^2 at the in-vivo stress level.

Another method of determining the Young's modulus is to use the local slope of the stress-strain curve. Using this definition the value of E is 9×10^6 dynes/cm^2. The large difference between these two values is due to the rapidly changing slope of the stress-strain curve at the level of the in-vivo stress.

The behavior of this curve deserves some further comment. It can be seen that near the origin the curve has a shallow slope and the associated E is in the neighborhood of 2×10^6 dynes/cm^2. As the strain is increased, the curve starts to increase its slope until at the in-vivo strain the corresponding E is 3×10^6 dynes/cm^2. Once this natural strain is exceeded the slope of the curve increases much more rapidly. Thus, with the vessel in its natural, stretched condition it becomes increasingly more difficult to raise the strain level a given amount.

This behavior is not unexpected when one looks at the classical description of the structure of the vessel wall. It has been postulated by Frasher (32) and others that there are basically 4 types of tissue present in the artery wall. The inner most lining is the endothelium, a thin layer of cells that is common to all vessels and is in intimate contact with the blood. Collagen is a protein substance which exists in

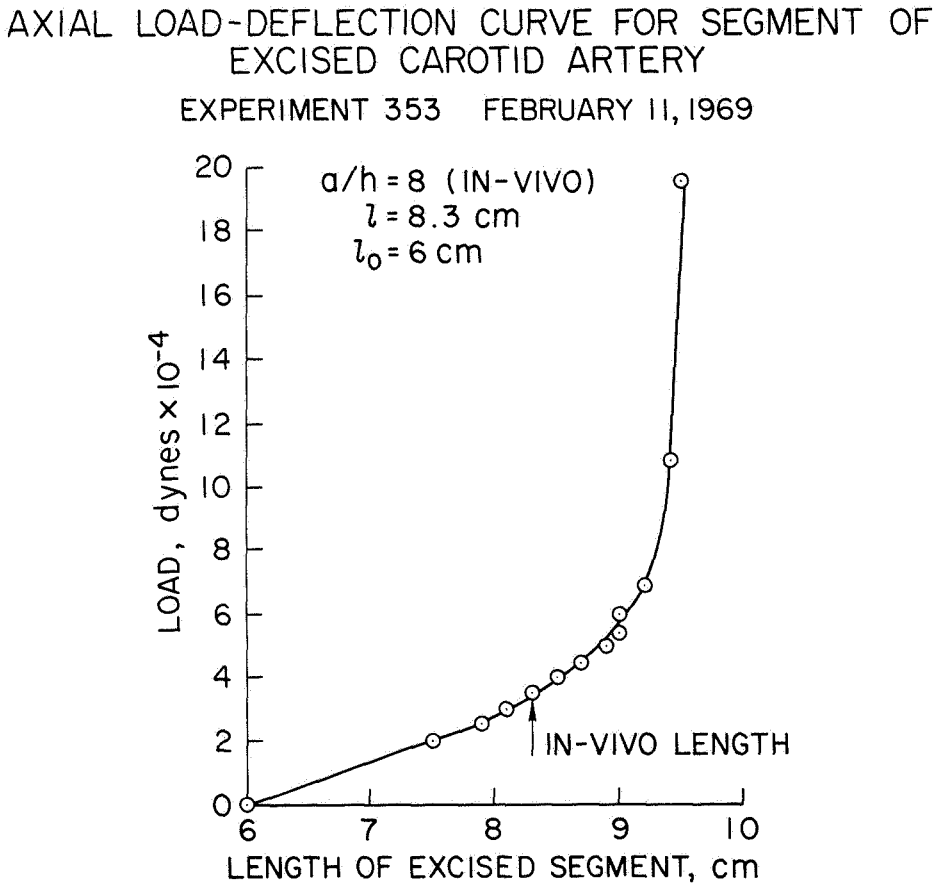

Figure 27. Load-elongation curve for a segment of excised carotid artery subjected to axial loading in a vertical test jig. The in-vivo stretch of the vessel is indicated.

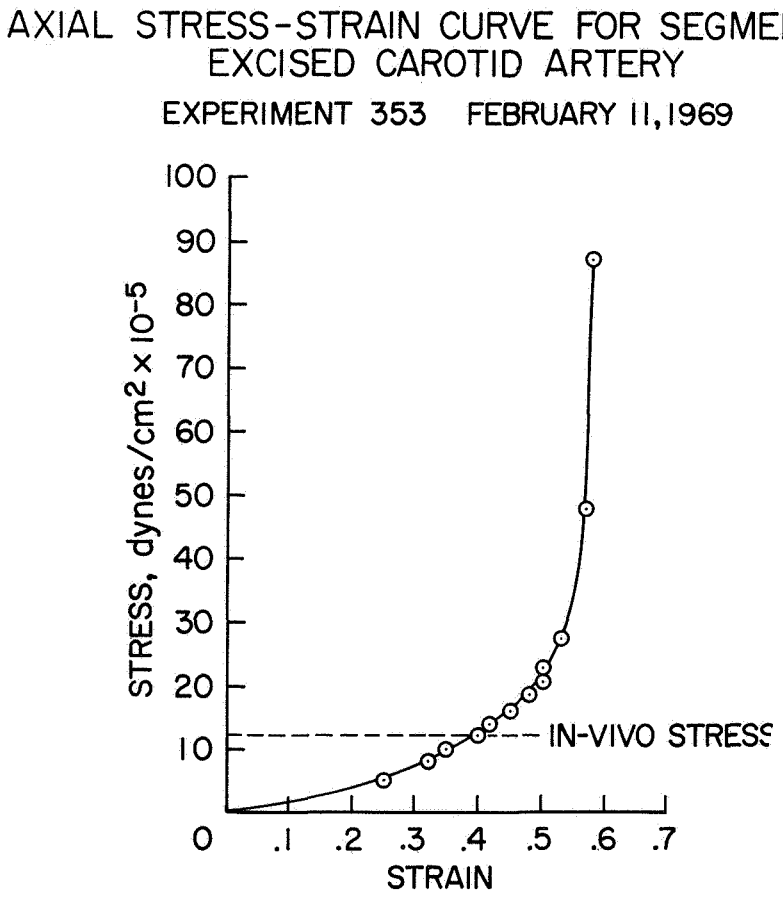

Figure 28. Stress-strain diagram for the segment of carotid artery used to determine the data shown in Figure 27. A Poisson's ratio of .5 was assumed and variations of the cross-sectional area of the vessel wall with stretch were accounted for in the analysis.

the vessel wall in long fibers and are bound together by a cement substance. It is estimated that the Young's modulus of collagen is approximately 10^8 dynes/cm^2. It is, incidentally, the principle component of tendons. Elastin is a second protein substance that has a low tensile strength and high extensibility with an $E = 6 \times 10^6$ dynes/cm^2. The final primary substance found in artery walls is smooth muscle. The Young's modulus of this material is dependent on the stimulus acting on it at the time. Bergel (31) has shown that the active tension measured after chemical stimulation yields an E of about 10^6 dynes/cm^2.

Burton (33) gives a description of what he believes to be the mechanism exhibited by the vessel wall when it is subjected to longitudinal stress. In the absence of active tension from the smooth muscle, increases in tension from near zero load are mainly taken up in the elastin fibers. This is because the collagen, even though much more rigid, is oriented randomly along the vessel axis. Once the collagen fibers become rearranged and are oriented along the vessel axis they begin to carry a greater share of the load. Thus, the behavior of the curves in Figures 27 and 28 is not unexpected (see also (30)).

Using the results of the stress-strain analysis carried out above, values of the stretch parameter q_1 were calculated for changes in strain of $\pm$ 10 percent around the naturally occurring strain. Regardless of the definition used to determine the value of the Young's modulus, such changes in strain resulted in at most a two fold increase in q_1 from - 10 percent to + 10 percent.

Therefore, on the basis of Maxwell and Anliker's analysis (13), one would not expect to see large changes in the transmission characteristics of the three types of waves in response to changes in the initial stretch of this magnitude.

In an effort to verify these conclusions, the stretch was varied about the naturally occurring length and the transmission characteristics of all three types of waves were measured.

Changing the stretch of the vessel was accomplished by simply moving the collar device which gripped the vessel in such a way as to increase or decrease the distance between the stations. Data was then taken on the dispersion and attenuation of the various types of waves. It was found that

increasing the stretch by .1 was not generally possible due in part to the very nature of the stress-strain curve. If we look at the curve in Figure 28 we see that an increase in strain of .1 beyond that naturally present would require about twice as much stress. In addition, as the vessel is stretched it contracts in the radial direction in order to maintain constant voloume. This decrease in diameter resulted in the artery slipping through the collar device. Thus even if we were able to approach increases of 10 percent in length we couldn't maintain them without virtually occluding the artery. Indeed, 5 percent increases in the length of the segment were sometimes difficult to maintain.

Due to these difficulties, data was generally taken on decreases in initial length. This was easily accomplished because the distal branches of the carotid artery (the ones toward the head) and their surroundings are more elastic than the long segment of the carotid artery in the exposed test section.

The fact that it was not possible to study the effects of large increases in the stretch should not be considered a severe limitation on the results given in this section. Increases in the length of the vessel which might be induced by natural motions of the head of the dog are probably accomodated by a shifting of the vessel within its tissue bed in such a way as to relieve most of the increased strain. While one carotid artery tends to be stretched as the animal turns its head to one side, the other tends to relax. Thus, one is more likely to encounter decreases in stretch than increases in the carotid artery under physiologically meaningful conditions.

All of the experiments described in this section were done on the exposed carotid artery.

Results

Presure Waves

Figure 29 shows the results of one experiment in which the stretch was varied a total of 16 percent (from an 8.5 percent decrease to a 7.4 percent increase in stretch) and the speed of the pressure waves were measured at various frequencies. While the curves show some inconsistency,

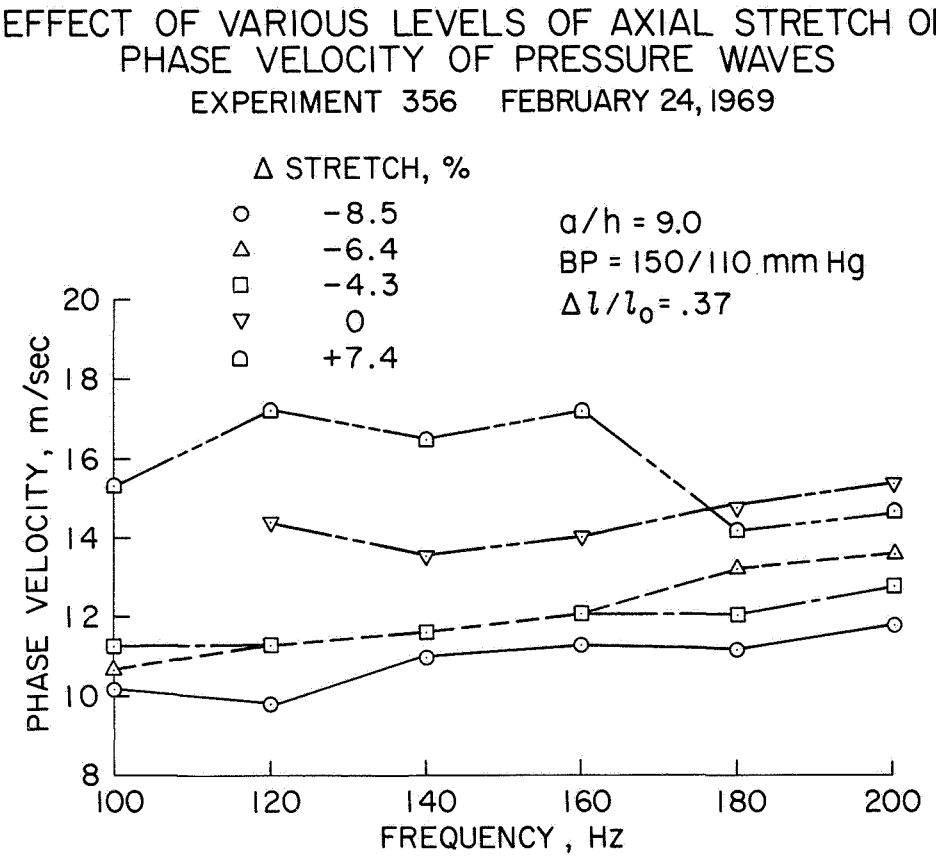

Figure 29. Phase velocity of artificially induced pressure waves as a function of frequency for various values of stretch. Each point represents the average of at least 5 velocity measurements.

the general pattern of increasing speed with increasing stretch prevails as well as the nondispersive nature found in Section B of this chapter. In particular, the speed is seen to increase from 11 m/sec at -8.5 percent up to 16.5 m/sec at +7.4 percent at 140 Hz. This same basic pattern was shown in two other experiments.

The varition of the damping of the pressure waves was not quite so well defined. In all cases, a decrease in stretch resulted in a slight decrease in damping. However, the data exhibited such a high degree of scatter that no quantitative conclusion may be made as to the effect of initial stretch on the damping of pressure waves in the carotid artery.

Torsion Waves

The effect of decreasing the stretch of the artery on the phase velocity of torsion waves is shown in Figure 30, where the results of two experiments are given. The large discrepency between the speed values for different dogs at the natural stretch (Δstretch = 0) reflects individual differences among the animals rather than variations in the initial strain. Table I shows that in one case the initial strain was .40 and in the other case .38.

The essential conclusion from the data must then be limited to saying that the speed of the torsion wave appears to be highly dependent on the initial stretch of the vessel. A decrease in that stretch will be reflected in a decrease in speed. The results of two other experiments tend to confirm this conclusion.

The damping of torsion waves as indicated by the value of k appears to be independent of the initial stretch over the range of values covered in these experiments.

Axial Waves

Changes in the transmission characteristics of axial waves in respons to varying initial stretch were similar to those found for torsion and pressure waves. As can be seen in Figure 31, as the stretch was decreased the phase velocity decreased rather markedly. For a frequency of 50 Hz, the velocity fell from approximately 27 m/sec to about 15 m/sec when the stretch was decreased a total of 12 percent.

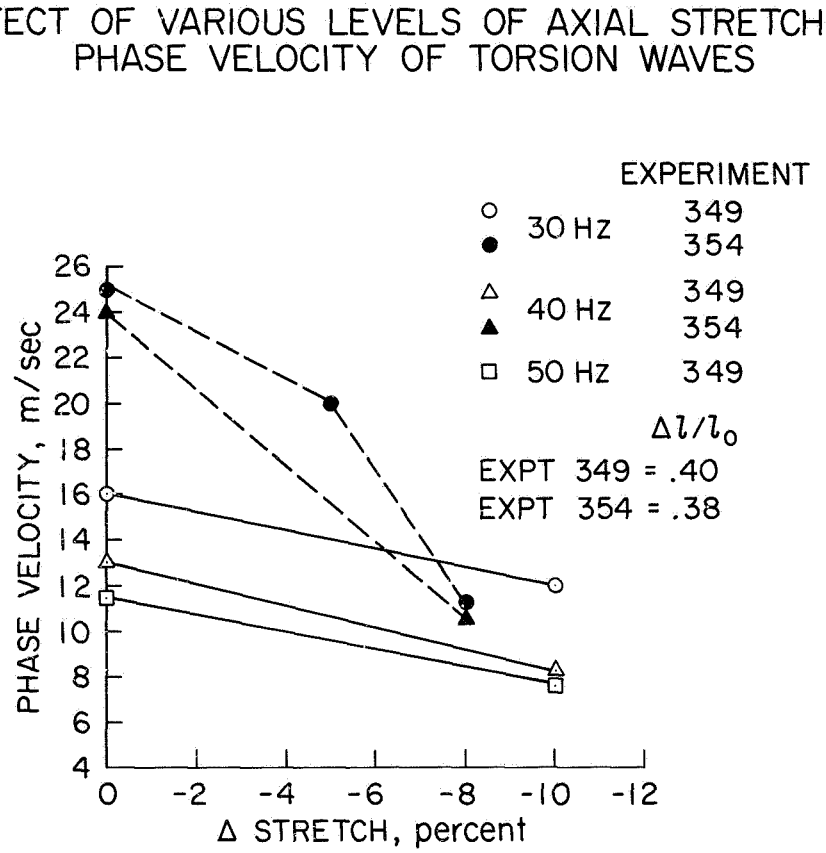

Figure 30. Phase velocity of torsion waves as a function of the stretch for 3 frequencies. The data obtained from 2 dogs is shown. The large difference in the speeds at zero Δstretch is probably due to individual variations between dogs. Each point represents the average of at least 5 velocity measurements.

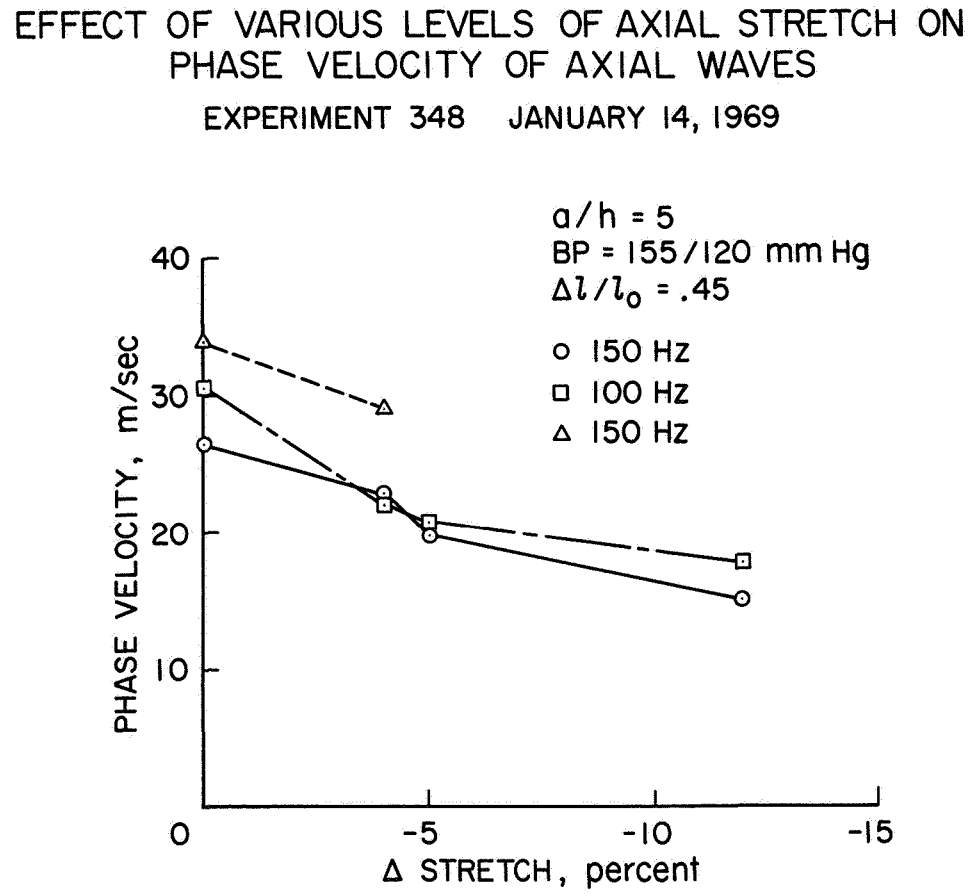

Figure 31. Phase velocity of axial waves as a function of stretch for 3 frequencies. The decrease in speed noted can be rougly correlated with changes in the Young's modulus in the axial direction as determined from the results shown in Figure 28. The results shown are typical of data obtained from 3 other dogs.

The most dramatic decrease in speed occurred at the values of Δstretch near zero. From Figure 28 we see that the slope of the stress-strain curve approaches a constant value as the strain is decreased from its in-vivo value. Thus, one would expect that with decreasing values of strain, the rate of change of the axial wave velocity would also decrease. Indeed, this appears to be the case as shown in Figure 31. Unfortunately, decreases in strain greater than 12 percent were not obtainable.

As was the case for both the pressure and torsion waves, the damping of axial waves was not markedly effected by changes in the initial stretch of the vessel over the range 0 to 12 percent. Indeed, virtually all the data from 4 animals showed no significant change in the attenuation in response to changes in strain.

Discussion

The phase velocity of all three types of waves is strongly dependent on the initial strain of the vessel. When this longitudinal strain is decreased the velocity of each wave decreases. The magnitude of this decrease is much greater than was predicted by the analysis in reference (13). However, when the stress-strain curve of a vessel segment is studied the behavior observed in this section is not at all unreasonable.

In fact, if the curve in Figure 28 is used and we note that a 12 percent decrease in strain results in a decrease of E from 9×10^6 to 2×10^6 dynes/cm^2 (measured tangentially), then decreases in speed on the order of 50 percent for the axial waves are to be expected. This conclusion is based on the assumption that the speed of the axial waves varies as the square root of E (12,13).

The attenuation of all three types of waves appears to be essentially uneffected when the initial strain is varied within the limits of the above experiments.

F. EFFECT OF SURROUNDING MEDIUM

Introduction

When the prospect of using a non-invasive technique to determine the mechanical properties of blood vessels using wave transmission studies is considered, the effect that the surrounding tissue may have on the dispersion and attenuation of the various waves is clearly of importance. Since all of the arteries and veins are in contact with their surroundings, one might expect to see some form of coupling between the vessel wall ahd its contiguous tissues.

Jones et al (14) have shown theoretically that axial waves are more sensitive to changes in the elestic properties of the surroundings than are the pressure waves. Their results indicate that, on the basis of their analysis and the assumptions made therein, the modulus of elasticity of the surrounding medium must be at least 3 orders of magnitude less than that of the vessel wall in order to produce negligible contrainst effects. On the other hand, it must be at least two orders of magnitude greater than that of the vessel in order to significantly effect pressure waves.

Experimental observations of the in-vivo tethering of the carotid artery in the neck of dogs indicate that the vessel is only mildly bound to its surroundings. The carotid artery lies in a triangular trough formed by the longus colli or longus capitis dorsally, the trachea ventromedially and the brachiocephalicus and sternocephalicus laterally. The internal jugular vein and the vagosympathetic nerve trunk are associated with the carotid artery in the middle of the neck. These structures are bound to the carotid artery and are attached to the surrounding medium by the carotid sheath. The sheath is part of the poorly developed deep cervical fascia that exists in this region of the neck (34).

Intuition, coupled with these anatomical considerations, then would lead one to expect that the transmission characteristics of the various types of waves should not be strongly effected by the presence of these surrounding tissues. A study was conducted to determine, in a given dog, just what changes in the dispersion and attenuation patterns resulted from the presence of the surrounding medium.

In each case, the structures adjacent to the carotid artery were

left undisturbed over various lengths in the mid-region of the neck while data was acquired on the transmission of the various waves through this region. The surrounding tissue was then removed and again data was taken using the same frequencies and amplitudes as before.

Results

Pressure Waves

In the case of pressure waves there is some inconsistency in the results. In two dogs, the surrounding medium served to increase the speed up to 20 percent over that found in the exposed vessel while in 4 other experiments the speed did not change in the presence of the surrounding tissue. This variation is probably attributable to differences between dogs or to differences in surgical trauma and anesthesia. Figure 32 shows the results of one experiment in which there was a marked increase in the speed while the dispersive nature of the pressure waves was not altered. The other 4 experiments gave results which showed a smaller rise in speed than that shown in Figure 32, which is representative of the results of the first two experiments mentioned.

The damping, on the other hand, was not significantly different. As can be seen from Figure 33, the attenuation in the presence of the surrounding medium was essentially the same as in the exposed case.

Torsion Waves

The effect of surrounding tissue on the transmission of torsion waves appears to be most dramatic. It was found that the fascia which surrounds the carotid artery completely damps out the induced torsion waves over a distance of less than 4 cm. In other words, with 4 cm of essentially undisturbed tissue around the vessel, no torsion waves could be detected at the distal station when the station closest to the shaker (proximal) was undergoing torsional wall motion on the order of 2 mm peak-to-peak. This result was independent of frequency in the range 20 to 100 Hz and was found in 5 dogs.

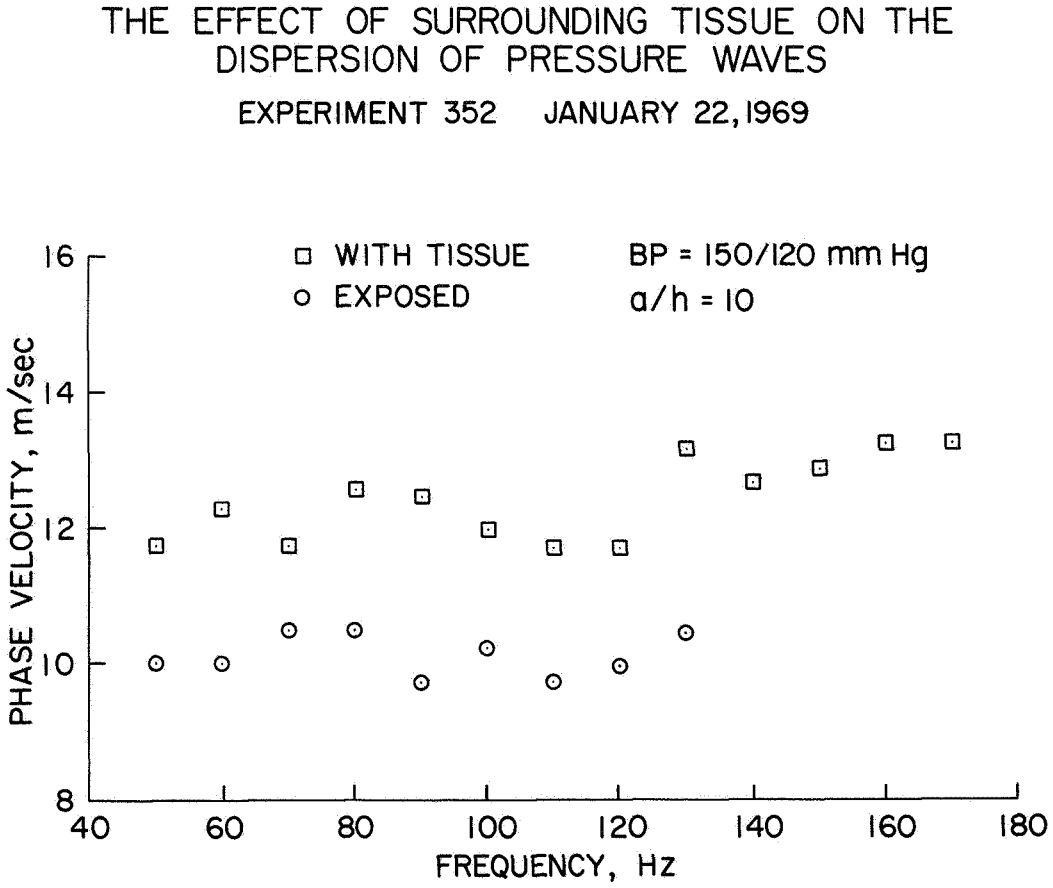

Figure 32. The effect of surrounding tissue on the dispersion of artificially induced pressure waves in the carotid artery. The results shown here represent the greatest difference observed between exposed and unexposed vessels in four dogs.

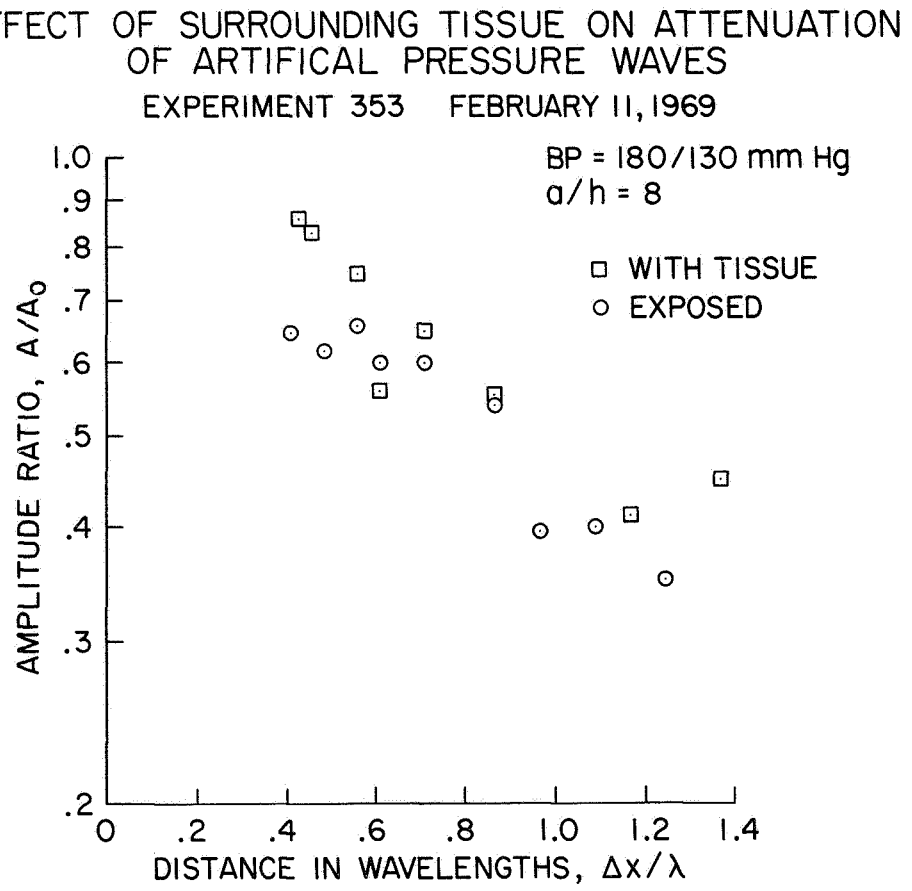

Figure 33. Typical results on the effect of surrounding tissue on the damping of artificially induced pressure waves in the carotid artery.

Axial Waves

The effect of the surrounding tissue on the phase velocity of axial waves is small and appears to vary between animals. Six experiments were conducted to study this effect. In two of them the phase velocity was definitely higher in the presence of the surrounding medium than in the exposed case while in the remaining four experiments there was essentially no difference in the speed as measured under the two conditions. In fact, in some cases the velocity was slightly less in the case of surrounding tissue than in the exposed case although the magnitude of these differences were within the experimental error associated with these measurements. The results of one experiment are shown in Figure 34. This experiment showed quite a marked change in the presence of the tissue. As in the case of pressure waves, the explanation of the differences noted between dogs is probably the result of individual variations and slightly different trauma.

The manner in which the tissue effects the damping of axial waves also appears to vary between dogs. In some experiments the damping was significantly higher in the presence of tissue than in the exposed case while in others the attenuation was essentially the same. Figure 35 shows the results of one experiment where the difference was particularly great. Note that instead of the data following an exponential decay pattern, it appears that a more complicated relationship exists between the amplitude ratio and the distance traveled in wavelengths. While the other experiments did not show a change in attenuation as large as that in Figure 35, the same change in shape was apparent in most of them.

Discussion

It seems that the following statements may be made regarding the effect of the surrounding tissue on the transmission characteristics of the three types of waves. The phase velocity of the pressure and axial waves appears to be at least mildly effected by the presence of the surrounding medium in some dogs while both waves do not show a consistent pattern between dogs. Torsion waves appear to be so strongly damped by the tissue that no quantitative statements can be made regarding the effect of the surrounding medium. The damping of pressure waves was not significantly effected while the attenuation of the axial waves appeared

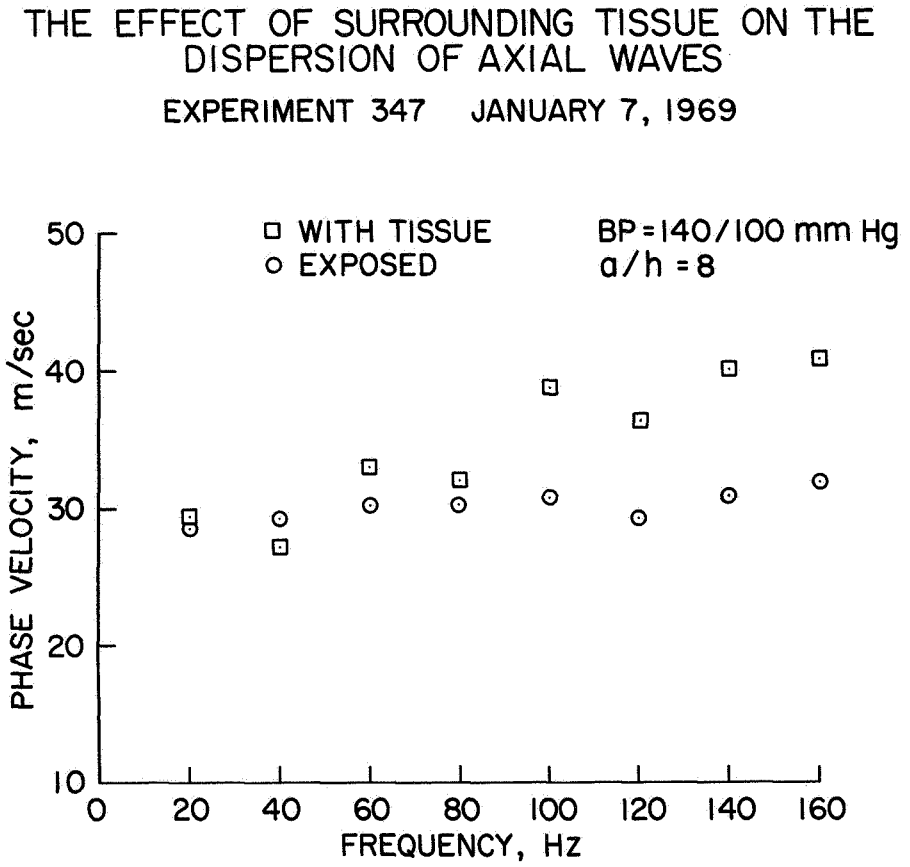

Figure 34. The effect of the surrounding medium on the dispersion of axial waves in the carotid artery. The results shown here represent the most marked difference between the exposed and unexposed case found in 6 dogs. Each point represents the average of at least 5 velocity measurements.

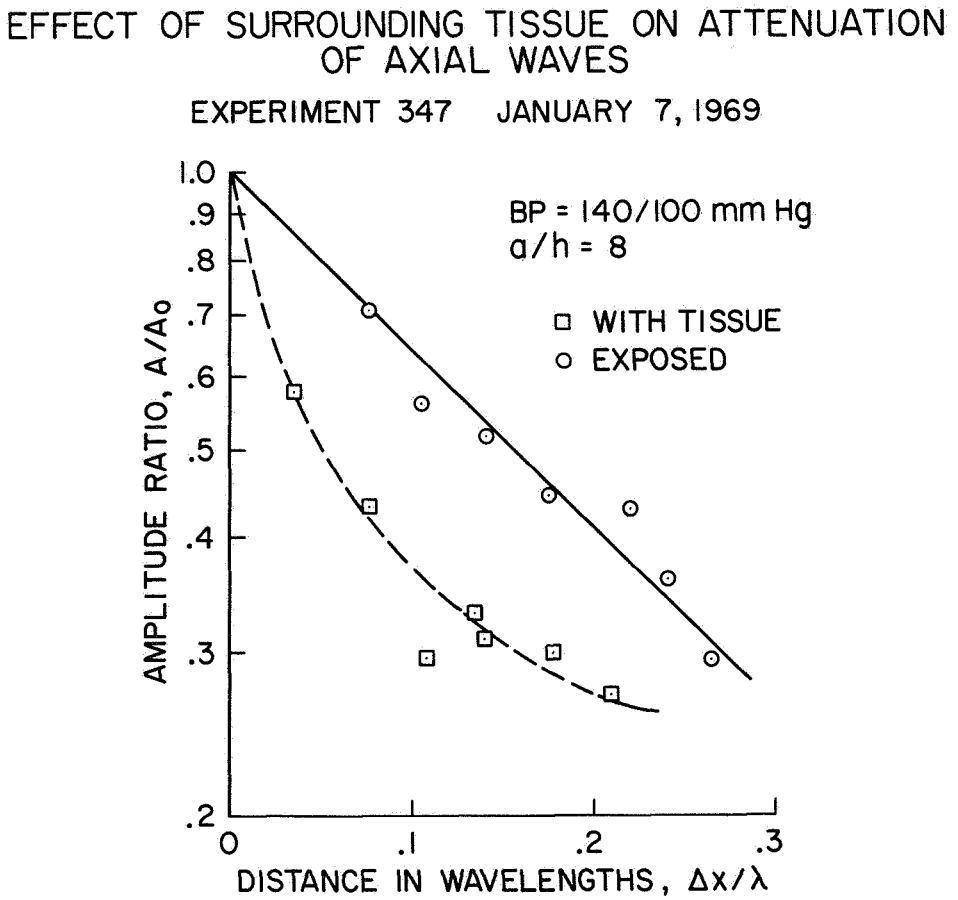

Figure 35. The effects of surrounding tissue on the attenuation of axial waves in the carotid artery. It appears that the surrounding tissue alters the exponential decay pattern observed in the exposed case.

to change shape and increase over that in the exposed case. These conclusions of course only apply over the frequency and amplitude ranges covered in these experiments.

VI. SUMMARY AND CONCLUSIONS

The application of wave transmission techniques to the study of the mechanical behavior of the carotid artery has been carried out in anesthetized dogs. The dispersion and attenuation of small amplitude distension (pressure), torsion and axial waves have been measured under various conditions. In addition, the components of the naturally occurring wall displacements were determined along with the speed of the natural pressure pulse wave in the carotid artery.

The velocity of propagation of the front of the natural pressure wave is between 8 and 13 m/sec depending on the transmural pressure. The higher speeds are associated with higher arterial pressures. At normal blood pressure levels the speed was found to average 10-11 m/sec. The presence of the surrounding tissue did not change these results.

In the case of the exposed vessel, there was no naturally occurring circumferential wall motion in the carotid artery that could be detected by the methods of data acquisition and analysis used herein. There was, however, a rather large axial wall displacement (.5 mm) which was made up of two components--one assooiated with the traveling pressure pulse wave and the other the result of motion of the heart within the chest cavity during the normal cardiac cycle. This latter component was highly damped and ceased to exist about 10 cm above the brachiocephalic while the pressure pulse component was present over the entire length of the carotid artery studied.

Increasing the transmural pressure had a dramatic effect on the phase velocity of small amplitude pressure waves. Raising the arterial pressure by 100 mm Hg would cause a 100 percent increase in the speed of the artificially induced pressure waves. This increase in speed appears to be the result of a change in the mechanical properties of the blood vessel in response to increased pressure rather than a flow effect. Torsion and axial waves showed little or no change in their transmission characteristics due to change in the transmural pressure.

The dispersion and attenuation of pressure and axial waves appear to be independent of the initial amplitude of the disturbance within the ranges covered in these experiments. The damping of torsion waves, on the

other hand, is quite dependent on A_o. Increasing A_o by a factor of three can increase A/A_o from .5 to .7. The phase velocity of torsion waves is virtually independent of A_o however.

The carotid artery in its natural state is subjected to a longitudinal stress which results in a strain of about .4. Changes in the level of axial strain have a significant effect on the dispersion of all three types of waves. In all cases, decreasing the initial stretch resulted in a decrease in the phase velocity. The amount of change varied with the level of strain. This result is not unexpected on the bais of the stress-strain tests made on a segment of excised artery. These results predict a lower value of Young's modulus at the decreased levels of strain. In fact, on the basis of a simplified expression for the speed of the axial wave, the decrease in velocity observed can be directly related to a decrease in the effective Young's modulus.

The effect of the surrounding medium on the transmission characteristics varies substantially between dogs. In some cases the speed of the axial and pressure waves was increased due to the surrounding medium and the transmission decreased (i.e. A/A_o became smaller at any $\Delta x/\lambda$) while in others there was no change. Torsion waves, on the other hand, were completely damped out over an unexposed distance of less than 4 cm.

The primary purpose of this research was to determine the dispersion and attenuation patterns for the three types of waves in the exposed carotid artery. The results indicate that the pressure wave is nondispersive and has a speed of about 11 m/sec while the torsion and axial waves are mildly dispersive with speeds that range between 15-24 and 25-35 m/sec, respectively, for frequencies between 20 and 100 Hz. The damping of all three types of waves appears to be independent of frequency and can be approximated by $A/A_o = \exp(-k\,\Delta x/\lambda)$. The range of the logarithmic decrements, k, for the various waves is: pressure--.8 to 1.5; torsion--4.0 to 6.5 (dependent on A_o); and axial--3.5 to 5.0.

When these results are compared with theoretical predictions based on various mathematical models for the mechanical behavior of arteries, it appears that the vessel wall behaves in a nonisotropic fashion. In fact, the carotid artery of the dog seems to be about twice as extensible in the axial than in the circumferential direction. While this conclusion has been

reached by other investigators working on segments of excised vessels, it has never been shown on in-vivo arteries. It is believed that the results given in this dissertation are the first in-vivo evidence for an anisotropic artery wall.

In addition, the large attenuation exhibited by the various waves is primarily the result of damping mechanisms in the vessel wall and point toward a viscoelastic behavior with high viscous damping.

It thus appears that in order to obtain a truly valid mathematical model for the mechanical behavior of blood vessels it will be necessary to account for the effects of anisotropy and high viscous damping in the vessel wall.

REFERENCES

1. Witzig, K., Über erzwungene Wellenbewegungen zäher, inkompressibler Flüssigkeiten in elastischen Röhren. Inaugural Dissertation, Universität Bern, Wyss 1914.

2. Iberall, A.S., Attenuation of Oscillatory Pressures in Instrument Lines, Journal of Research, National Bureau of Standards. Research Paper RP2115, Vol. 45, July 1950, pp. 85-108.

3. Morgan, G.W. and Kiely, J.P., Wave Propagation in a Viscous Liquid Contained in a Flexible Tube, J. Acoust. Soc. Am., Vol. 26, No. 3, May 1954, pp. 323-328.

4. Womersley, J.R., An Elastic Tube Theory of Pulse Transmission and Oscillatory Flow in Mammalian Arteries, WADC Technical Report TR 56-614, Wright Air Development Center, Ohio, Jan. 1957.

5. Hardung, V., Propagation of Pulse Waves in Viscoelastic Tubings, Handbook of Physiology, Circulation, Vol. 1, Am. Physiol. Soc., 1962, pp. 107-135.

6. Klip, Willem, Velocity and Damping of the Pulse Wave, Martinus Nijhoff, The Hague, 1962.

7. McDonald, D.A., Blood Flow in Arteries, Edward Arnold Ltd., London, 1960.

8. Fox, E.A., and Saibel, Edward, Attempts in the Mathematical Analysis of Blood Flow, Trans. Soc. Rheol. VII, 1963, pp. 25-31.

9. Rudinger, G., Review of Current Mathematical Methods for the Analysis of Blood Flow, Biomedical Fluid Mechanics Symposium, 1966, ASME, New York, pp. 1-33.

10. Skalak, R., Wave Propagation in Blood Flow, Biomechanics, App. Mech. Div., ASME, Ed. Y.C. Fung, 1966, pp. 20-40.

11. Fung, Y.C., Biomechanics, Its Scope, History and Some Problems of Continuum Mechanics in Physiology, J. App. Mech. Reviews, Vol. 21, No. 1, Jan. 1968, pp. 1-20.

12. Anliker, M. and Maxwell, J.A., The Dispersion of Waves in Blood Vessels, Biomechanics Symposium, ASME, New York, 1967, pp. 47-67.

13. Maxwell, J.A. and Anliker, M., The Dissipation and Dispersion of Small Waves in Arteries and Veins with Viscoelastic Wall Properties, Biophysical J., Vol. 8, No. 8, 1968, pp. 920-950.

14. Jones, E., Chang, I-Dee and Anliker, M., Effects of Viscosity and External Constraints on Wave Transmission in Blood Vessels, SUDAAR Report No. 344, Department of Aeronautics and Astronautics, Stanford University, Stanford, California, 1968.

15. Wells, M. K., On the Determination of the Elastic Properties of Blood Vessels from Their Wave Transmission Characteristics, SUDAAR Report No. 368, Department of Aeronautics and Astronautics, Stanford University, Stanford California, 1969.

16. Attinger, E.O., Ed., Pulsatile Blood Flow: Proceedings, Blakiston Division, McGraw-Hill Book Co., New York, 1964.

17. Dick, D., Kendrich, J., Matson, G. and Rideout, V.C., Measurement of Non-linearity in the Arterial System of the Dog by a New Method, Cir. Res. 22, Feb. 1968, pp. 101-111.

18. Anliker, M., Histand, M.B., and Ogden, E., Dispersion and Attenuation of Small Artificial Pressure Waves in the Canine Aorta, Cir. Res. 23, Oct. 1968, pp. 539-551.

19. Landowne, Milton, A Method Using Induced Waves to Study Pressure Propagation in Human Arteries, Cir. Res., Vol. V, Nov. 1957, pp. 594-601.

20. Landowne, Milton, Characteristics of Impact and Pulse Wave Propagation in Brachial and Radial Arteries, J. App. Physiol. 12(I), 1958, pp. 91-97.

21. Peterson, Lysle H., The Dynmanics of Pulsatile Blood Flow, Cir. Res., Vol II, March 1954, pp. 127-139.

22. Anliker, M., Wells, M.K. and Ogden, E., The Transmission Characteristics of Large and Small Pressure Waves in the Abdominal Vena Cava, to appear in the IEEE Transactions on Biomedical Engineering Devoted to the Venous System.

23. Patel, D. and Fry, D., The Elastic Symmetry of Arterial Segments in Dogs, Cir. Res., Vol XXIV, January 1969, pp. 1-8.

24. Histand, M.B., An Experimental Study of the Transmission Characteristics of Pressure Waves in the Aorta, SUDAAR Report No. 369, Department of Aeronatics and Astronautics, Stanford University, Stanford, California, 1969.

25. Atabek, H.B. and Lew, H.S., Wave Propagation through a Viscous Incompressible Fluid Contained in an Initially Stressed Elastic Tube, Biophysical Journal, Vol. 6, 1966, pp. 481-503.

26. Klip, W., Van Loon, P. and Klip, D., Formulas for Phase Velocity and Damping of Longitudinal Waves in Thick-Walled Viscoelastic Tubes, J. App. Physics, Vol. 38, No. 9, August 1967, pp. 3745-3755.

27. Patel, D., Mallos, A and Fry, D., Aortic Mechanisms in the Living Dog, J. Appl. Physiol., 16(2), 1961, pp. 293-299.

28. Patel, D. and Fry, D., Longitudinal Tethering of Arteries in Dogs, Cir. Res., Vol. XIX, Dec.1966, pp. 1011-1021.

29. Fenn, W.O., Changes in Length of Blood Vessels on Inflation, Tissue Elasticity, Ed. J.W. Remington, Am. Physiol. Soc., 1957, pp. 154-160.

30. King, A.L., Some Studies in Tissue Elasticity, Tissue Elasticity, Ed. J.W. Remington, Am. Physiol. Soc., 1957, pp. 123.

31. Bergel, D., The Static Properties of the Arterial Wall, J. Physiol., 156, 1961, pp. 445-457.

32. Frasher, W., What is Known about the Physiology of Larger Blood Vessels, Biomechanics Symposium, ASME, New York, 1967, pp. 1-19.

33. Burton, A., Physiology and Biophysics of the Circulation, Year Book Medical Publishers, Chicago, 1965.

34. Miller, M.E., Anatomy of the Dog, W.B. Saunders Co., 1964.